View metadata, citation and similar papers at core.ac.uk
brought to you by CORE
provided by D-Scho

A TRANSIENT MODEL FOR INSULATED GATE BIPOLAR TRANSISTORS (IGBTs)

By

Mohsen A Hajji

B.S. in E.E., University of Pittsburgh, 1988

M.S. in E.E., University of Pittsburgh, 1996

Submitted to the Graduate Faculty

of the school of Engineering

In partial fulfillment of

the requirement for the degree of

Doctor

of

Philosophy

University of Pittsburgh

2002

The author grants permission
to reproduce single copies.

Signed ______________________________

COMMITTEE SIGNATURE PAGE

This dissertation was presented

by

Mohsen A. Hajji

It was defended on

July 31, 2002

and approved by

(Signature) ____

Committee Chairperson
Mahmoud El Nokali, Associate Professor

(Signature) ____

Committee Member
Dietrich Langer, Professor

(Signature) ____

Committee Member
Amro El-Jaroudi, Associate Professor

(Signature) ____

Committee Member
George Kusic, Associate Professor

(Signature) ____

Committee Member
Patrick Smolinski, Associate Professor

ABSTRACT

A TRANSIENT MODEL FOR INSULATED GATE BIPOLAR TRANSISTORS (IGBTs)

Mohsen A. Hajji, Ph.D.

University of Pittsburgh, 2002

The Insulated Gate Bipolar Transistor is widely accepted as the preferred switching device in a variety of power converters and motor drive applications. The device combines the advantages of high current density bipolar operation that results in low conduction losses with the advantages of the fast switching and low drive power of MOSFET gated devices. The basic idea behind IGBT is to increase the conductivity of a thick lightly doped epitaxial layer, thus reducing the on-resistance and losses associated with power MOSFET. This reduction in resistivity resulting from high level of carrier injection is referred to as conductivity modulation. When the IGBT is turned OFF, however, injected carriers must be extracted first before the device can sustain the reverse blocking

voltage. Several models have been proposed in the literature to describe both DC and transient behaviors of IGBTs. These models can be broadly classified into two main categories: physics based models and behavioral or compact models. The dissertation compares the various approaches made in the literature to model the transient behavior of IGBTs. A new physics-based model for a Non Punch Through (NPT) IGBT during transient turn OFF period is presented. The steady state part of the model is derived from the solution of the ambipolar diffusion equation in the drift region of the IGBT. The transient component of the model is based on the availability of a newly developed expression for the excess carrier distribution in the base. The transient voltage is obtained numerically from this model. Alternatively, an analytical solution for the transient voltage is presented. The theoretical predictions of both approaches are found to be in good agreement with the experimental data. The model is used to calculate the instantaneous power dissipation $P(t)$ and the switching losses E_{off} in an IGBT for different device carrier lifetimes.

DESCRIPTORS

High-level injection | Non-Punch Through IGBT

Ambipolar Diffusion Equation | Analytical Modeling

Physics-based model | Transient Turn-OFF Losses

ACKNOWLEDGMENTS

I take this opportunity to deeply thank my advisor, Prof. Mahmoud El Nokali, for helping me establish a strong foundation in the physics of IGBT power device. Working under his supervision, I learned how to be responsible, organized and self-dependent. His innovative thinking and outstanding teaching policy were highly stimulating. May God always bless him, his family and relatives.

I would like to thank Dr. Dietrich Langer, Dr. Amro El-Jaroudi, Dr. George Kusic and Dr. Patrick Smolinski for being my Ph.D. committee members. Also, my thanks go to Dr. H.K. Ahn for his time and valuable guidance.

I am thankful to my family and my country for supporting me in various ways. I am also thankful to the chairman of the Electrical Engineering Department Professor Joel Falk for his help and support.

TABLE OF CONTENTS

Page

ABSTRACT ……………………………………………………………….iii

ACKNOWLEDGMENTS ……………………………………………………v

LIST OF TABLES …………………………………………………….....ix

LIST OF FIGURES ……………………………………………………..x

NOMENCLATURE…………………………………………………....xiii

1.0 INTRODUCTION………………………………………………….....1

2.0 BASIC BACKGROUND……………………………………………….6

2.1 IGBT Structure…………………………………………………….6

2.2 IGBT Operation…………………………………………………..11

2.3 Basic Tools For The Analysis……………………………………12

2.3.1 The Steady State Condition……………………………...13

2.3.2 Transient Operation of IGBT……………………………18

3.0 LITERATURE REVIEW ANALYSIS OF SOME TRANSIENT MODELING OF IGBT……………………………………………………21

4.0 A NEW PHYSICS-BASED TRANSIENT MODEL……………………...32

4.1 The Steady State…………………………………………………32

4.2 Turn-OFF Transient……………………………………………...34

4.2.1 Expression For $\frac{dV_{CE}(t)}{dt}$ …………………………………35

4.2.2 The Instantaneous Power $P(t)$ and Switching Losses $E_{off}(t)$ ……………………………………………...51

4.2.3 An Alternative Analytical Solution For The Transient $\frac{dV_{CE}(t)}{dt}$ ……………………………..58

5.0 RESULTS AND DISCUSSION……………………………………65

6.0 SUMMARY AND FUTURE WORK…………………………...69

APPENDIX A **LINEAR CHARGE CONTROL**………72

APPENDIX B $\frac{I_T(0^+)}{I_T(0^-)}$ **EXPRESSION IN CASE** $I_n(W) = 0$………………………………..75

APPENDIX C $\frac{I_T(0^+)}{I_T(0^-)}$ **EXPRESSION IN CASE** $I_n(W) \neq 0$………………………………...77

APPENDIX D **DERIVATION OF AN ANALYTICAL SOLUTION FOR THE** $\frac{dV_{CE}(t)}{dt}$……...79

BIBLIOGRAPHY……………………………………………………86

LIST OF TABLES

Table No. **Page**

1 IGBT Model Parameters……………………………………………………49

2 Physical Parameters……………………………………………………...50

LIST OF FIGURES

Figure No. **Page**

1. A cross section schematic of the IGBT half-cell…………………………7

2. Equivalent circuit model of the IGBT…………………………………….8

3. 1-D coordinate system used in the modeling of the NPT IGBT…………15

4. Typical IGBT turn-OFF transient showing turn-OFF phases (1 and 2)…20

5. The collector-base capacitance formation………………………………..22

6. Adjusted coordinate system used for Ramamurthy IGBT analysis [5]….31

7. The steady state charge Q_0 as a function of carrier lifetime τ_{HL}…………44

8. Linear excess carrier concentration profile as a function of $W(t)$………45

9. Comparison of anode voltages with experimental data for different lifetimes……………………………………………………………………..46

10. Large inductive loads with no freewheeling diode in an IGBT circuit….47

11. Inductive loads with a free wheeling diode in an IGBT circuit…………48

12. The instantaneous power dissipated by the IGBT for different lifetimes for the numerical model……………………………………………………..52

13. E_{off} as a function of time for $\tau_{HL} = 0.3\mu S$ ……………………………...53

14. E_{off} as a function of time for $\tau_{HL} = 2.45\mu S$ …………………………….54

15. E_{off} as a function of time for $\tau_{HL} = 7.1\mu S$ ………………………………55

16. Comparison of the energy losses for three different lifetimes in an IGBT

for the numerical model……………………………………………………56

17. Turn-OFF switching losses (E_{off}) as a function of anode current for the numerical model…………………………………………………………57

18. Comparison of anode voltages with different lifetimes between the analytical model and experimental data………………………………...61

19. Anode current profiles…………………………………………………..62

20. Comparison of anode voltages with the reference model for different lifetimes……………………………………………………………………63

21. $a_{\max}$ values for different lifetimes for NPT IGBT structure…………….64

22. $\left(\frac{I_T(0^+)}{I_T(0^-)}\right)$ output as a function of the bus voltage and lifetime through the ratio of $\left(W(t)/L\right)$ ……………………………………………………..83

23. Saber software simulation for $I_T(0^+)$ as a function of V_{bus} and τ_{HL} …...84

NOMENCLATURE

A	Device active area (cm^2).
$b = \frac{\mu_n}{\mu_p}$	Ambipolar mobility ratio.
μ_n, μ_p	Electron, hole mobility ($\frac{cm^2}{VS}$).
D_n, D_p	Electron, hole diffusivity ($\frac{cm^2}{S}$).
D	$= \frac{2D_n D_p}{(D \ + D_p)}$, Ambipolar diffusivity ($\frac{cm^2}{S}$).
I_n, I_p	Electron, hole current (A).
I_{sne}	Emitter electron saturation current (A).
I_T	Device anode current (A).
N_B	Base doping concentration (cm^{-3}).
q	Electronic charge (1.6×10^{-19} C).
Q	Total excess carrier base charge(C).
Q_0	Steady-state base charge (C).
P_0	Excess carrier concentration at $x = 0(cm^{-3})$.
$p(x)$	Excess carrier concentration (cm^{-3}).
τ_{HL}	Base high-level lifetime (S).

L	$=\sqrt{D\tau_{HL}}$, Ambipolar diffusion length (cm)
ε_{si}	Dielectric constant of silicon (F/cm)
x	Distance in base from emitter (cm).
W_B	Metallurgical base width (cm).
$W(t)$	Collector-base depletion width (cm).
C_{bcj}	$=\frac{A\varepsilon_{si}}{W_{bcj}(t)}$, Collector-base depletion capacitance (F).
$V_{CE}(t)$	Device anode voltage (V).

1.0 INTRODUCTION

The Insulated Gate Bipolar Transistor (IGBT) is a power-switching device that combines power MOSFET input characteristics with bipolar output characteristics. This device is controlled at the input by MOSFET voltage; however, the output current is characteristic of that of a bipolar junction transistor (BJT). Consequently, the device is called an insulated gate bipolar transistor (IGBT). The combination of the low on state resistance of power bipolar transistor and the high input impedance of power MOSFET is one of the advantages of this device. The high input impedance of power MOSFET allows controlled turn-on and gate controlled turn-OFF[1] [1].

Several models have been proposed in the literature to describe both the DC and the transient behaviors of the IGBT. These models can be classified into two categories: physics-based and behavioral (compact) models.

The model outlined in this thesis dissertation belongs to the category of physics-based models in that the basic semiconductor physics of the IGBT device is used to develop relations between the excess minority carrier's distribution, the anode current (I_T), the base current and the output voltage of the device ($V = V_{CE} = V_{BC}$). There are no exact solutions when considering physics-based modeling approach. Appropriate mathematical representations should be found to roughly approximate the solution. It is possible to reach an exact solution if certain assumptions are met when considering the imposed boundary conditions. The analytical modeling approach uses parameters, which

[1] Bracket references placed in the front of the line of text refer to bibliography.

have physical meanings and are related to each other based on the device physics. Nevertheless, developing a physical model is time consuming. Since there are some simplifying approximations made when developing a physics-based model, accuracy may not be 100%. Furthermore, different structures of the IGBT device or new devices require new modifications or new models.

The analytical model developed by Hefner et al. [2-3] is the most comprehensive in the category of physics-based IGBT model.

Trivedi et al. [4] provided a numerical solution to obtain $\frac{dV(t)}{dt}$ in terms of the total current I_T during the turn-OFF for hard and soft switching IGBT application. The sweeping out action of the excess carriers in the drift region due to the widening of the collector-base depletion was used to obtain $\frac{dV(t)}{dt}$ expression. Since $W(t)$ decreases or shrinks due to the widening of the depletion region in the collector-base, the charges are forced to be taken away and $I_h = qp(x)\upsilon(x) = qp(x)\frac{dW(t)}{dt}$.

Ramamurthy et al. [5] proposed an analytical expression for the voltage variation with time $\frac{dV(t)}{dt}$ for the turn-OFF of the IGBT. The simple expression for the variation of the internal charges and the boundary conditions with voltages is a non-linear one. For the turn-OFF analysis, Ramamurthy linearized the steady state carrier concentration expression $p(x)$. Ramamurthy used a positive value for $\frac{dW(t)}{dt}$ instead of a negative sign, which contradicts the equality $W(t) = W_B - W_{bcj}(t)$.

Fatemizadeh et al. [6] developed a semi-empirical model for IGBT in which the DC and the transient current transport mechanisms of the device were approximated by simple analytical equations. The model equations of the IGBT were installed on the PSPICE simulator using analog behavioral modeling tools. However, the accuracy of the model is limited by the fact that the analytical semi-empirical model is over simplified.

Yue et al. [7] presented an analytical IGBT model for the steady state and transient applications including all levels of free carrier injection in the base region of the IGBT. The authors have shown that the low and high injection models significantly overestimate the IGBT current at large and small bias conditions respectively.

Kraus et al. [8] considered an NPT IGBT with a higher charge carrier lifetime and lower emitter efficiency. The injection of electrons into the emitter of the IGBT instead of carrier recombination in the base determined the I-V characteristics. The anode hole currents and the emitter hole currents are assumed constant. Due to his neglection of the recombination in the base, a linear charge distribution instead of the hyperbolic function was derived.

Kuo et al. [9] derived an analytical expression for the forward conduction voltage (V_F) for NPT and PT IGBTs taking into account the conductivity modulation in the base of the IGBT. The MOSFET section has not been included in the analysis. Since I_{MOS} controls the turn-OFF process of the IGBT, the MOSFET section should have been included.

Sheng et al. [10] solved the two dimensional (2-D) carrier distribution equations to model the forward conduction voltages, which can be used in circuit simulation and

device analysis for (DMOS IGBT). The drawback of this modeling approach is that it contains complex terms that would impose some requirements on the simulator.

Sheng et al. [11] reviewed IGBT models published in the literature; he then analyzed, compared and classified models into different categories based on mathematical type, objectives, complexity and accuracy. Although [11] claimed that many mathematical models are accurate and able to predict electrical behavior in different circuit conditions compared to the behavioral models, it failed to provide a comprehensive physical model for understanding the device mechanisms.

Leturcq [12] proposed a simplified approach to the analysis of the switching condition in IGBT. The approach was based on a new method for solving the ambipolar diffusion equation taking the moving depletion boundary in the base into consideration. This paper helped in understanding the switching process in IGBT.

The above literature survey dealt mainly with IGBT having planar structures, namely the Non-Panch Through (NPT) and the Punched Through (PT) IGBT, although other structures were proposed in the literature to improve the I-V characteristics of IGBTs, temperature operation or develop better physics-based models [13-23].

This Ph.D. dissertation deals with modeling the transistor I-V characteristics of the IGBT device during the switching or turning-OFF period. Chapter 2 describes the basic structure of an IGBT and provides a description of the IGBT operation. In addition, the chapter introduces the ambipolar transport analysis, which is the key feature in modeling the IGBT device. The conclusion of the chapter highlights the basic tools for the analysis: the steady state and the transient operation of an IGBT. Chapter 3 covers the literature review analysis of the most important transient modeling of IGBT. Chapter 4

introduces new physics-based models for NPT IGBT wherein the steady state part of the model is derived by solving the ambipolar diffusion equation in the base. The turn-OFF transient part of the model is based on the availability of a new expression for excess carrier charge distribution in the base. The transient voltage is obtained numerically from this model. Alternatively we have proposed and implemented an analytical solution for the transient voltage. In addition, the power dissipation $P(t)$ and the switching losses E_{off} in IGBT are calculated and simulated for different device carrier lifetimes.

Chapter 5 discusses the output results for voltage, current, power dissipation and energy losses.

Chapter 6 provides a summary of the work accomplished and possible future research area applications.

2.0 BASIC BACKGROUD

2.1 IGBT Structure

Figure 1 shows a cross section schematic of a typical IGBT. Figure 2 shows the discrete equivalent circuit model of the device, which consists of a wide base P-N-P bipolar transistor (BJT) in cascade with a MOSFET. The structure of the device is similar to that of a vertical double diffused MOSFET with the exception that a highly doped p-type substrate is used in lieu of a highly doped n-type drain contact in the vertical double diffused MOSFET. A lightly doped thick n-type epitaxial layer ($N_B \approx 10^{14} cm^{-3}$) is grown on top of the p-type substrate to support the high blocking voltage in the reverse bias mode state. A highly doped p-type region ($N_A \approx 10^{19} cm^{-3}$) is added to the structure to prevent the activation of the PNPN thyristor during the device operation. The power MOSFET is a voltage-controlled device that can be manipulated with a small input gate current flow during the switching transient. This makes its gate control circuit simple and easy to use.

A highly doped n^+ buffer layer could also be added on top of the highly doped $p+$ substrate. This layer helps in reducing the turn-OFF time of the IGBT during the transient operation. The IGBT with a buffer layer is called a punch through PT
IGBT while the IGBT without a buffer layer is named a non-punch through NPT IGBT.

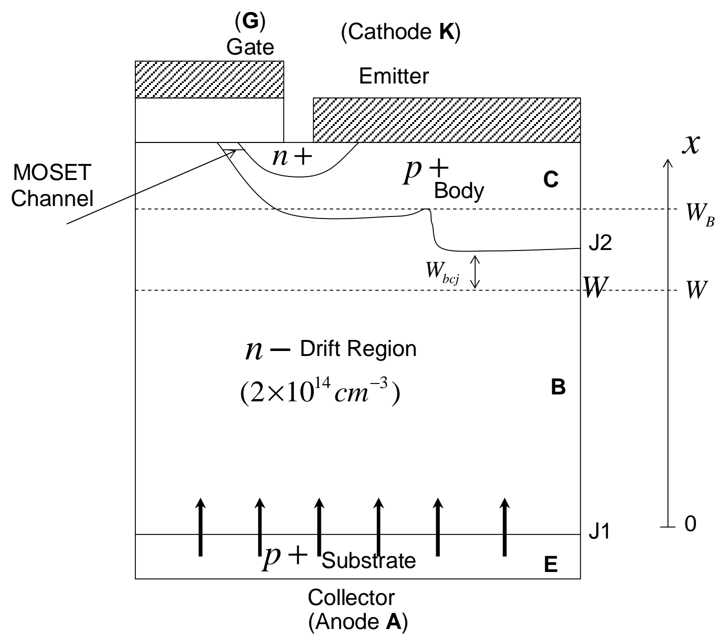

Figure 1 A cross section schematic of the IGBT half-cell.

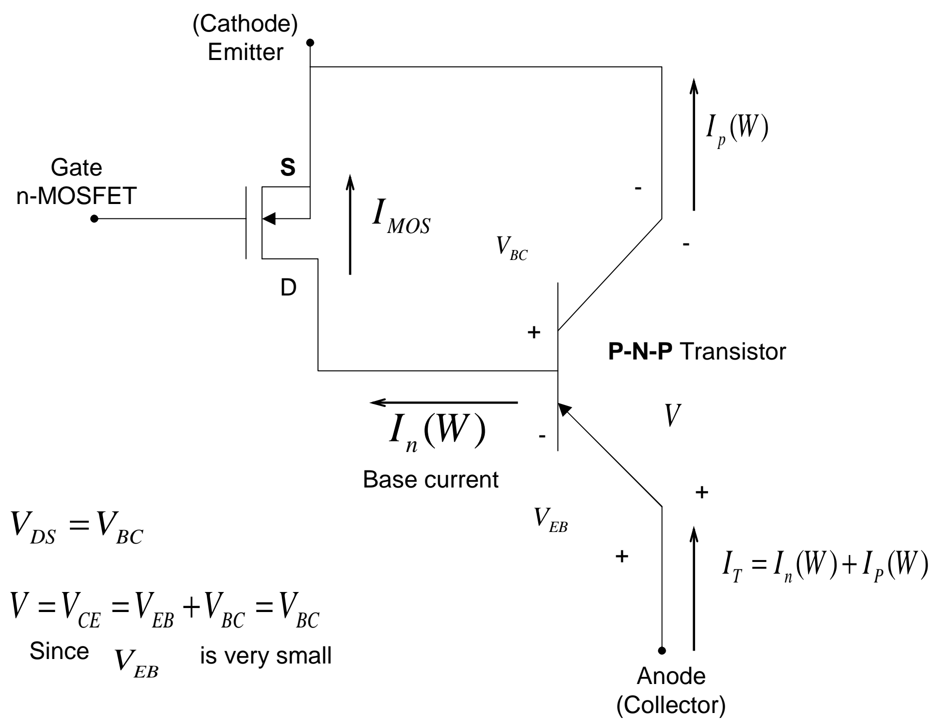

Figure 2 Equivalent circuit model of the IGBT.

In the case of PT IGBT, the epilayer is not as thick (less thick) as NPT IGBT because a n^+ layer is placed over the $p+$ layer. It is very likely to have punched through the J2 junction to the J1 junction. This n^+ layer can handle some of the punch through and act as a shield to the J1 junction. This n^+ buffer layer occupies some spaces in the base of IGBT, which leaves less space for the total charges in the base region during the IGBT on state (turn-on) operation. As a result, these charges are removed by the n^+ layer more quickly when switching occurs. This n^+ layer is a recombination center which helps holes get recombined with electrons before reaching the base region and fewer holes, as a result, will be injected into the base region (lower efficiency). As a result, the carrier lifetime is reduced and the switching frequency is increased. However, since fewer carriers are injected into the base region compared to the NPT IGBT, the conductivity modulation (explained later) is reduced (higher base resistance) and the on-state voltage is increased. The trade OFF between the reduced turn-OFF time and the increased on-state voltage should be accounted for.

For NPT IGBT considered in this thesis dissertation, the epilayer thickness is thick enough since no n^+ layer is introduced on top of the highly doped $p+$ layer substrate. Because the thickness of the n^- layer is greater than PT IGBT, the resistance is high in this region and, as a result, a higher reversed voltage can be sustained when J2 is reversed biased. The punch through of the J2 to the J1 is less likely to occur, i.e. a non-punch through situation. If the punch through occurs, then the IGBT breakdown voltage will be degraded causing the device to break down. When the emitter base junction J1 is

forward biased and the gate voltage is greater than the threshold voltage V_T; injection of holes from the $p+$ substrate is increased. The resistance of the n- layer is reduced when the injected hole density becomes much greater than the background doping ($n^- = N_B$). The turn-OFF time of the NPT IGBT is longer than the PT IGBT because the removal of so many stored charges in the base region is slow due to the absence of recombination centers. Carriers do not recombine as fast, which means they have longer lifetimes. The NPT IGBT is more efficient than the PT ones since more charges are injected from the $p+$ layer to the n^-. The injected holes do not get recombined as fast as in PT IGBT, which has an n^+ buffer layer on top of the $p+$ layer.

2.2 IGBT Operation

When a positive gate voltage greater than the threshold voltage (V_T) is applied, electrons are attracted from the $p+$ body towards the surface under the gate. These attracted electrons will invert the $p+$ body region directly under the gate to form an n channel. A path is formed for charges to flow between the n^+ source and the n^- drift region.

When a positive voltage is applied to the anode terminal of the IGBT, the emitter of the IGBT section is at higher voltage than collector. Minority carriers (holes) are injected from the emitter ($p+$ region) into the base (n^- drift region). As the positive bias on the emitter of the BJT part of the IGBT increases, the concentration of the injected hole increases as well. The concentration of the injected holes will eventually exceed the background doping level of the n^- drift region; hence the conductivity modulation phenomenon. The injected carriers reduce the resistance of the n^- drift region and, as a result, the injected holes are recombined with the electrons flowing from the source of the MOSFET to produce the anode current (on state).

When a negative voltage is applied to the anode terminal, the emitter-base junction is reversed biased and the current is reduced to zero. A large voltage drop appears in the n^- drift region since the depletion layer extends mainly into that region.

The MOSFET gate voltage controls the IGBT switching action. The turn-OFF takes place when the gate voltage is less than the threshold voltage (V_T). The inversion layer at the surface of the $p+$ body under the gate cannot be kept and therefore no

electron current is available in the MOSFET channel while the remaining minority carriers of holes, which were stored during the on state of the IGBT, require some time in order to be removed or extracted.

The switching speed of the IGBT device depends upon the time it takes for the removal of the stored charges in the n^- drift region which were built up during the on state current conduction (IGBT turn-on case).

2.3 Basic Tools For The analysis

The physics-based modeling approach is used in this dissertation to better understand the effect of the carriers on the IGBT characteristics. The following points have to be taken into account in performing the analysis:

1. The carrier distribution in the n-drift region of the IGBT is described by the ambipolar diffusion equation because of the high level injection of holes in this region ($p(x) \rangle\rangle N_B$):

$$\frac{\partial^2 p(x)}{\partial x^2} = \frac{p(x)}{L^2} + \frac{1}{D}\frac{\partial p(x)}{\partial t}$$

where N_B is the base background doping concentration, $p(x)$ is the hole concentration, $L = \sqrt{D\tau_{HL}}$ is the ambipolar diffusion length, D is the ambipolar diffusion constant and τ_{HL} is the hole carrier lifetime.

2. The transport of the bipolar charge is assumed to be one-dimensional (1-D) for the ease of analysis.

3. The emitter region of the BJT part of the IGBT has a very high doping concentration level ($p+\rangle\rangle\ 10^{18}cm^{-3}$). This region also acts like recombination centers for minority carriers coming from the lightly doped base region (electron in this case).

4. The space charge region, which is depleted of minority carriers, supports the entire voltage drop across the collector-base terminals based on Poisson's equation. The effect of mobile carriers in the depletion region is not accounted for in this dissertation.

2.3.1 The Steady State Condition

The equivalent circuit model and 1-D coordinate system of Figure 3 is used in the modeling approach of the NPT IGBT analysis. From this Figure, I_T is the IGBT total current, I_p is the hole current of the BJT and I_n is the base or MOS electron current.

I_T can be expressed in several ways:

$$I_T = I_p(x=0) + I_n(x=0)$$

$$I_T = I_p(x=W) + I_n(x=W)$$

$$I_T = I_p(x) + I_n(x).$$

The IGBT operates under low gain and high-level injection conditions. The current equations are given as

$$J_n = nq\mu_n E + qD_n \frac{\partial n(x)}{\partial x} \tag{2-1}$$

$$J_p = pq\mu_p E - qD_p \frac{\partial p(x)}{\partial x} \tag{2-2}$$

where J_n and J_p are the electron and hole current densities respectively.

The first terms in equations (2-1) and (2-2) are due to the drift component while the second terms are due to the diffusion component.

When the excess carrier concentration is larger than the background concentration, the transport of electrons and holes are coupled by the electric field in the drift terms of the transport equations. The minority carrier current density J_n cannot be neglected and ends up affecting the majority carrier current density J_p. Hence, equations (2-1) and (2-2) cannot be decoupled.

The total current density is given by

$$J_T = J_n + J_p = (nq\mu_n + pq\mu_p)E + q\left[D_n \frac{\partial n}{\partial x} - D_p \frac{\partial p}{\partial x}\right].$$

Substituting for the electric field from the above equation into equation (2-1) yields

$$J_n = \left[\frac{nq\mu_n}{nq\mu_n + pq\mu_p}\right] J_T + q\frac{\partial n}{\partial x}\left[\frac{nq\mu_n D_p + pq\mu_p D_n}{nq\mu_n + pq\mu_p}\right].$$

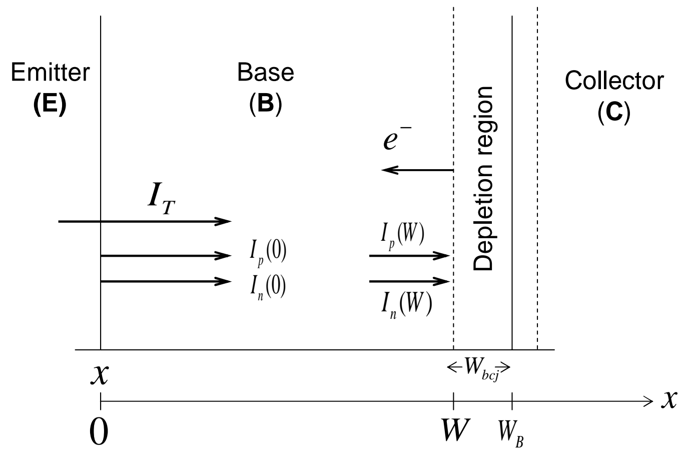

Figure 3 1-D coordinate system used in the modeling of the NPT IGBT.

An ambipolar diffusion coefficient D is defined as

$$D = \frac{nq\mu_n D_p + pq\mu_p D_n}{nq\mu_n + pq\mu_p} .$$

The expression for J_n can be rearranged and rewritten as

$$J_n = \frac{b}{1+b} J_T + qD\frac{\partial n}{\partial x} \tag{2-3}$$

where $b = \mu_n / \mu_p$.

Repeating the same procedure starting with equation (2-2), J_p is obtained

$$J_p = \frac{1}{1+b} J_T - qD\frac{\partial p(x)}{\partial x} \tag{2-4}$$

where J_T is the total current density = $J_n + J_p$.

The excess hole carrier distribution $p(x)$ can be obtained by solving the steady state hole continuity equation

$$\frac{\partial^2 p(x)}{\partial x^2} = \frac{p(x)}{L^2} \tag{2-5}$$

Considering the coordinate system given in Figure 3, the boundary conditions for the excess hole carrier distributions are [2]

$$p(x = W) = 0 \tag{2-6}$$

$$p(x = 0) = P_0 \tag{2-7}$$

Equation (2-6) results from the collector-base junction being reversed biased for forward condition and equation (2-6) reflects the fact that the emitter-base junction is forward biased.

P_0 is the excess carrier concentration at $x = 0$, $W(t)$ is the quasi-neutral base width given by

$$W = W_B - W_{bcj} \tag{2-8}$$

where W_B is the metallurgical base width and W_{bcj} is the collector-base depletion width.

Solving Poisson's equation (2-9) yields an expression for the collector-base junction depletion width as in equation (2-10)

$$\frac{d^2V}{dx^2} = \frac{qN_B}{\varepsilon_{si}} \tag{2-9}$$

$$W_{bcj} = \sqrt{\frac{2\varepsilon_{si}V_{bc}}{qN_B}} \tag{2-10}$$

where N_B is the doping concentration of the lightly doped region of the IGBT and ε_{si} is the dielectric constant of silicon. The junction voltage $V_{bcj} = V = V_{bc} + V_{bi}$, V_{bc} is the collector-base junction voltage drop of the BJT part of the IGBT and V_{bi} is the built in potential. Hence from Figure 2

$$W = W_B - \sqrt{\frac{2\varepsilon_{si}V}{qN_B}} \tag{2-11}$$

where $V = V_{bc} = V_{CE} = V_A$ is the collector-base voltage that appears across the drift region.

2.3.2 Transient Operation of IGBT

While the turn-on time of the IGBT is quite fast, the turn-OFF time can be slow because of the open base of the PNP transistor during the turn-OFF period. Figure 4 shows the typical IGBT turn-OFF transient where $I_T(0^-)$ is the on-state current before the initial rapid fall and $I_T(0^+)$ is the current after the initial rapid fall. The initial rapid drop in the anode current is due to the sudden removal of the MOS channel. This is followed by a slower decay due to the removal of the carriers stored in the lightly doped layer (n^-). The turn-OFF process is initiated when we lower the gate voltage to a value lower than the threshold voltage (V_T) (first phase). This removes the formed electron channel from under the gate and blocks the MOS component of the current I_{MOS}. $I_{MOS} = I_n(W) = 0$ in this case and the collector-base voltage V_{bc} increases resulting in a widening of the depletion region at the n^- (base-collector side or source of MOSFET).

The relation between $I_T(0^-)$ and $I_T(0^+)$ is through β_{tr} [2]. It is the ratio of the current immediately after the initial rapid fall to the magnitude of the fall and is shown along with the ratio of $W(t)$ to L $(W(t)/L)$ in the appendices.

The switching losses of the IGBT are dominated by the losses, which occur during the much slower second phase of the turn-OFF period transient. This is because of the time required removing or extracting the injected carriers in this phase. This is a

major disadvantage of the IGBT device as it suffers from high-switching losses. This can be overcome by reducing the lifetime of the carriers in the base through recombination or extraction processes as quickly as possible before the device reaches its blocking voltage state.

The collector-base junction is reversed biased and its depletion region widens during the turn-OFF of the IGBT. When the IGBT is on, the status of the base-collector junction is reversed biased as can be seen from Figure 2. When the IGBT is OFF, the status of the base-collector junction is reversed biased and V_{bc} is increased leading to the increment of the depletion region since the current decreases. The widened region supports the entire voltage drop across the device as mentioned previously based on Poisson's equation.

Since the quasi-neutral base width of the IGBT changes with time and decreases with the increase of V_{bc}, we can find an expression for the rate of rise of the voltage across the device $\frac{dV(t)}{dt}$ (varying of the output voltage) during the switching-OFF of the IGBT from the collector-base junction depletion width W_{bcj} expression as shown.

From $W_{bcj}(t) = \sqrt{\frac{2\varepsilon_{si} V_{bc}(t)}{qN_B}}$ and the fact that $W(t) = W_B - W_{bcj}(t)$ if we take the time derivative of $W_{bcj}(t)$, we get

$$\frac{dW_{bcj}(t)}{dt} = \sqrt{\frac{\varepsilon_{si}}{2qN_B V(t)}} \frac{dV(t)}{dt}$$

and $$\frac{dW(t)}{dt} = -\frac{dW_{bcj}}{dt} = -\sqrt{\frac{\varepsilon_{si}}{2qN_B V(t)}}\frac{dV(t)}{dt} \qquad (2\text{-}12)$$

This equation shows the time rate of change of the quasi-neutral base width ($W(t)$) that covers almost all the length across the drift region during the turn-OFF since the collector-base junction is reversed biased.

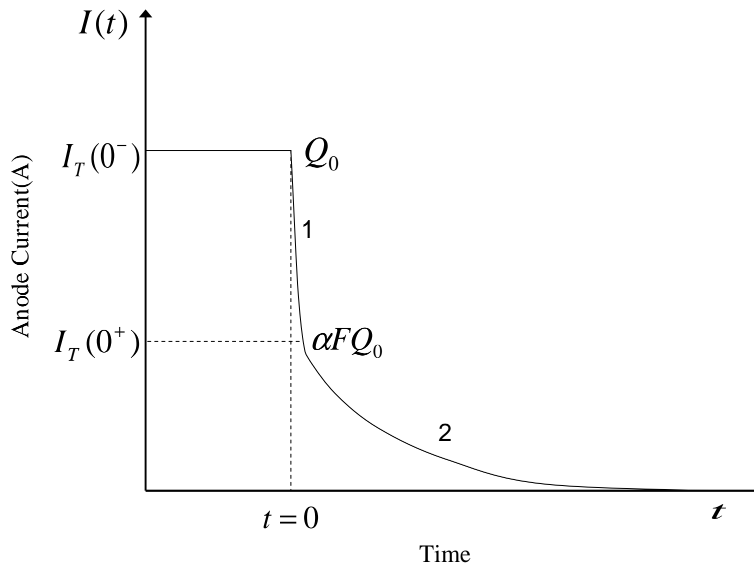

Figure 4 Typical IGBT turn-OFF transient showing turn-OFF phases (1 and 2).

3.0 LITERATURE REVIEW ANALYSIS OF SOME TRANSIENT MODELING OF IGBT

In Hefner et al. [3] transient modeling approach, the general ambipolar transport electron current expression ($I_n(W(t)) = \frac{I_T(t)}{\left(1+\frac{1}{b}\right)} + qAD\frac{\partial n(x)}{\partial t}$) was used to find an expression for the voltage rise ($\frac{dV(t)}{dt}$). $I_n(W(t)) = I_{MOS}$ as shown in Figure 3 and it is important since it controls the operation of IGBT. Since the reverse bias on junction J_2 in Figure 1 does not increase rapidly and the depletion capacitance of junction J_2 is partially charged in a short period of time, I_{MOS} current is instantaneous. An expression for I_{MOS} can be obtained if we consider the collector-base junction depletion capacitance as in Figure 5. For the voltage $V(t)$ between the plates, the charge per unit area $q = \frac{\varepsilon_{si}V(t)}{d}$, where d is the distance between the plates and the rate of q change is

$$\frac{dq}{dt} = I(current)$$

$$\because \quad q(t) = C_{bcj}(t)V(t)$$

$$\therefore \frac{dq}{dt} = \frac{d}{dt}(C_{bcj}(t)V(t))$$
$$= V(t)\frac{dC_{bcj}(t)}{dt} + C_{bcj}(t)\frac{dV(t)}{dt}$$

and in terms of the junction capacitance of the reverse biased junction, the displacement current $I_n(W(t))$ is

$$I_n(W) = V(t)\frac{dC_{bcj}(t)}{dt} + C_{bcj}(t)\frac{dV(t)}{dt}. \qquad (3\text{-}1)$$

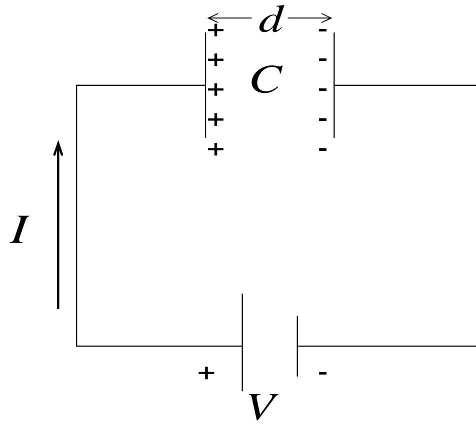

Figure 5 The collector-base depletion capacitance formation**.**

The first term on the right hand side of equation (3-1) was ignored by Hefner. The rate of change of $C_{bcj}(t)$ should be included in calculating the displacement current since the capacitance varies with time as the depletion width changes with voltage [25]. From equation (2-3) and the fact that $J = \frac{I}{A}$, where A is the device active area

$$I_n(W(t)) = \frac{b}{1+b} I_T(t) + AqD \frac{\partial p(x)}{\partial x}$$

and from Hefner's approach

$$I_n(W(t)) = C_{bcj}(t) \frac{dV(t)}{dt} = \frac{I_T(t)}{1+\frac{1}{b}} + \frac{2qAD_p}{1+\frac{1}{b}} \left. \frac{\partial p(x)}{\partial x} \right|_{x=W(t)}$$

$$(1+\frac{1}{b}) C_{bcj}(t) \frac{dV(t)}{dt} = I_T(t) + 2qAD_p \left. \frac{\partial p(x)}{\partial x} \right|_{x=W(t)} \qquad (3\text{-}2)$$

Hefner used equation (3-2) to obtain $V(t)$ for the transient operation of IGBT. He implemented the concept of moving the redistribution current. In his transient approach, he neither used the steady state expression for $p(x)$ (shown later) nor did he linearize the steady state expression for $p(x)$.

His $p(x)$ expression consists of two parts

$$p(x) = P_0 \left[1 - \frac{x}{W(t)} \right] - \frac{P_0}{W(t)D} \left[\frac{x^2}{2} - \frac{W(t)x}{6} - \frac{x^3}{3W(t)} \right] \frac{dW(t)}{dt} \qquad (3\text{-}3)$$

From equations (2-3) and (3-3)

$$I_n(W(t)) = \frac{bI_T(t)}{1+b} + qAD\frac{\partial p(x)}{\partial x}\bigg|_{x=W(t)}$$

$$I_n(W(t)) = \frac{I_T(t)}{1+\frac{1}{b}} + \frac{2qAD_p}{1+\frac{1}{b}}\frac{\partial p(x)}{\partial x}\bigg|_{x=W(t)} \tag{3-4}$$

and instead of equation (3-1), Hefner applied $I_n(W(t)) = C_{bcj}(t)\frac{dV(t)}{dt}$ in his approach.

Integrating equation (3-3) in the base and multiplying by qA, the total charge Q

$$Q = qA\int_0^W p(x)dx$$

$$= qA\left[x - \frac{x^2}{2W(t)}\right] - \frac{P_0}{W(t)D}\left[\frac{x^3}{6} - \frac{W(t)x^2}{12} - \frac{x^4}{12W(t)}\right]\frac{dW(t)}{dt}\bigg|_0^{W(t)}$$

$$= qA\left[P_0(W(t) - \frac{W(t)}{2})\right] - \frac{P_0}{W(t)D}\left[\frac{W^3(t)}{6} - \frac{W^3(t)}{12} - \frac{W^3(t)}{12}\right]\frac{dW(t)}{dt}$$

$$= \frac{qAP_0W(t)}{2} - \frac{qAP_0}{WD}\times 0$$

$$Q = \frac{qAP_0W(t)}{2} \tag{3-5}$$

as can be seen $\frac{dW(t)}{dt}$ has no effect on Q calculation.

We can find $\frac{\partial p(x)}{dx}\bigg|_{x=W(t)}$ from equation (3-3) as

$$\frac{\partial p(x)}{\partial x}\bigg|_{x=W(t)} = \frac{P_0}{W(t)} - \frac{P_0}{W(t)D}\left[\frac{2x}{2} - \frac{W(t)}{6} - \frac{3x^2}{3W(t)}\right]\frac{dW(t)}{dt}\bigg|_{x=W(t)}$$

$$\frac{\partial p(x)}{\partial x} = \frac{-P_0}{W(t)} - \frac{P_0}{W(t)D}\left[W(t) - \frac{W(t)}{6} - W(t)\right]\frac{dW(t)}{dt}$$

$$\frac{\partial p(x)}{\partial x} = \frac{-P_0}{W(t)} + \frac{P_0}{6D}\frac{dW(t)}{dt}$$

The hole current is $-qA\frac{\partial p(x)}{\partial x}$ [3] and from the above equation

$$-qAD\frac{\partial p(x)}{\partial x} = \frac{qADP_0}{W} - \frac{qADP_0}{6D}\frac{dW(t)}{dt}$$

$$= \frac{qADP_0}{W(t)} - \frac{qAP_0}{6}\frac{dW(t)}{dt}$$

$$\because Q = \frac{qAW(t)P_0}{2}$$

$$\therefore -qAD\frac{\partial p(x)}{\partial x} = \frac{2QD}{W^2(t)} - \frac{Q}{3W(t)}\frac{dW(t)}{dt} \tag{3-6}$$

The first term on the right hand side of equation (3-6) is categorized by Hefner as the charge control component and the second term is categorizes as the moving boundary redistribution component of the hole current.

From equations (3-4) and (3-6)

$$I_n(W(t)) = C\frac{dV(t)}{dt} = \frac{I_T(t)}{1+\frac{1}{b}} - \frac{4QD_p}{\left(1+\frac{1}{b}\right)W^2(t)} - \frac{2Q}{3W(t)}\frac{dW(t)}{dt}.$$

This equation can be expressed in a different way if $-qAD\frac{\partial p(x)}{\partial x}$ in equation (3-6) is modified as

$$-qAD\frac{\partial p(x)}{\partial x} = \frac{-2qAD_p}{\left(1+\frac{1}{b}\right)}\frac{\partial p(x)}{\partial x} = \frac{2QD}{W^2(t)} - \frac{Q}{3W(t)}\frac{dW(t)}{dt}$$

$$-2qAD_p\frac{\partial p(x)}{\partial x} = \frac{2QD}{W^2(t)}\left(1+\frac{1}{b}\right) - \frac{Q}{3W(t)}\left(1+\frac{1}{b}\right)\frac{dW(t)}{dt}$$

$$-2qAD_p\frac{\partial p(x)}{\partial x} = \frac{4D_pD_nQ}{W^2(t)\left(D_p+D_n\right)}\left(1+\frac{1}{b}\right) - \frac{Q}{3W(t)}\left(1+\frac{1}{b}\right)\frac{dW(t)}{dt}$$

$$-2qAD_p \frac{\partial p(x)}{\partial x} = \frac{4D_p Q}{W^2(t)} - \frac{Q}{3W(t)}\left(1+\frac{1}{b}\right)\frac{dW(t)}{dt}. \quad (3\text{-}7)$$

From equation (3-4), we have

$$I_n(W(t)) = C\frac{dV(t)}{dt} = \frac{I_T(t)}{1+\frac{1}{b}} + \frac{2qAD_p}{1+\frac{1}{b}}\left.\frac{\partial p(x)}{\partial x}\right|_{x=W(t)}$$

this can be rearranged as

$$\left(1+\frac{1}{b}\right)C(t)\frac{dV(t)}{dt} = I_T(t) + 2qAD_p\left.\frac{\partial p(x)}{\partial x}\right|_{x=W(t)}.$$

Now using equation (3-7), and the fact that

$$C(t) = C_{bcj}(t) = \frac{A\varepsilon_{si}}{W_{bcj}(t)} = A\sqrt{\frac{2\varepsilon_{si}N_B}{2V(t)}} \text{ and } \frac{dW(t)}{dt} = \frac{-C}{qAN_B}\frac{dV(t)}{dt},$$

the above equation yields

$$\left(1+\frac{1}{b}\right)C_{bcj}(t)\frac{dV(t)}{dt} = I_T(t) - \frac{4D_p Q(t)}{W^2(t)} - \frac{Q(t)}{3W(t)}\left(1+\frac{1}{b}\right)\frac{dW(t)}{dt}$$

$$C_{bcj}(t)\frac{dV(t)}{dt}\left[1+\frac{Q(t)}{3qAW(t)N_B}\right] = \frac{I_T(t) - \frac{4D_p Q(t)}{W^2(t)}}{\left(1+\frac{1}{b}\right)}$$

$$\frac{dV(t)}{dt} = \frac{\left[I_T(t) - \frac{4D_p}{W^2(t)}Q(t)\right]}{C_{bcj}(t)\left(1+\frac{1}{b}\right)\left[1+\frac{Q(t)}{3qN_B AW(t)}\right]} \quad (3\text{-}8)$$

where $I_T(t) \approx I_T(0^-)$ for large inductive loads and $I_T(t) = \frac{4D_p}{W^2(t)}Q(t)$ [Appendix A]

for the constant anode voltage in which $\frac{dV(t)}{dt} = 0$ indicating that the voltage and $W(t)$

are constants. Equation (3-8) is Hefner's transient $\frac{dV(t)}{dt}$ model for IGBT and $Q(t)$ is expressed by solving the following non-linear Hefner differential equation

$$\frac{dQ(t)}{dt} \approx -\frac{Q(t)}{\tau_{HL}} - \frac{4Q^2(t)I_{sne}}{W^2(t)A^2q^2n_i^2} \tag{3-9}$$

where I_{sne} is the emitter electron saturation current (A) and n_i is the intrinsic carrier concentration (cm^{-3}).

In Hefner's approach, the negative of the collected hole current $I_p(W(t))$ consists of a charge control current (I_{CC}) and redistribution current (I_R), which make this model more complex. The Expression $\frac{dQ(t)}{dt} \approx -\frac{Q(t)}{\tau_{HL}} - \frac{4Q^2(t)I_{sne}}{W^2(t)A^2q^2n_i^2}$ is not simple and Q_0 cannot be easily determined since there is no expression for P_0 which can be substituted for in Q_0 equation to evaluate Q_0 magnitude. Also, this model did not consider the rate of change of $C(t)$ in the calculation of the displacement current $I_n(W(t))$.

Trivedi et al. [4] applied the steady state carrier distribution equation ($p(x) = P_0 \frac{sinh[(W-x)/L]}{sinh(W/L)}$) for analyzing the turn-OFF process in the IGBT to derive the $\frac{dV(t)}{dt}$ expression. The net current following into the collector of the IGBT is

$$I_C = I_T = I_h + \beta_{pnp} I_h = \frac{I_h}{1-\alpha_{pnp}} \tag{3-10}$$

where I_h =BJT base current similar to $I_n(W)$ in equation (3-2), $\beta_{pnp} I_h$ =BJT collector current similar to $I_p(W)$ in Hefner's approach and $\alpha_{pnp} = sech\left(\frac{W}{L}\right)$ [1].

From equation (3-10), $I_h = qp(x)\upsilon(x) = qp(x)\frac{dW(t)}{dt}$ and $\frac{dW(t)}{dt}$ expression, $\frac{dV(t)}{dt}$ was obtained as

$$\frac{dV(t)}{dt} = \frac{2D_p cosh\left(\frac{W}{L}\right)\left(1 - sech\left(\frac{W}{L}\right)\right)I_T(t)}{I_T(0^-)Lsinh\left[\left(\frac{W-x}{L}\right)\right]}\sqrt{\frac{2qN_B V(t)}{\varepsilon_{si}}}e^{\left(t/\tau_{HL}\right)} \tag{3-11}$$

$e^{\left(-t/\tau_{HL}\right)}$ was added to take care of the decay of charges due to the recombination in the drift region. Trivedi et al. [4] multiplied τ_{HL} in the exponent term by a constant κ to account for the effect of both carrier recombination and electron current injection I_{sne}. This approach of multiplying κ with τ_{HL} alters the real value of τ_{HL}. The modeling approach for the $\frac{dV(t)}{dt}$ in [4] is different from Hefner's approach due to different key assumptions and equations used for the ambipolar electron and hole currents to analyze the turn-OFF process in the IGBT. This model ignored the diffusion effects of the carriers in the quasi-neutral base in the IGBT analysis besides using a positive expression for $\frac{dW(t)}{dt}$ which should be negative since ($W(t) = W_B - W_{bcj}(t)$).

Ramamurthy et al. [5] used different coordinate systems for modeling the transient turn-OFF of IGBT as shown in Figure 6 (i.e. $W = x$ and $W_B = d_1$). The steady state carrier distribution equation ($p(x) = P_0 \frac{sinh[(W-x)/L]}{sinh(W/L)}$) was applied to find P_0 expression.

P_0 was calculated from the total diffusion current density J_T with the use of boundary conditions for electron currents J_n, the hole current J_p and the total current J_T as

$$J_p(x = W = 0) = J_p \tag{3-12}$$

$$J_n(x = W = 0) = J_T(x = W = 0) - J_p(x = W = 0) \tag{3-13}$$

$$J_T(x = W = 0) = J_n(x = W = 0) + J_p(x = W = 0)\,. \tag{3-14}$$

From equations (3-12) to (3-13) and the expression for $J_n = \dfrac{J_T}{\left(1+\dfrac{1}{b}\right)} + qD\dfrac{\partial p(x)}{\partial x}$, P_0 is expressed as

$$P_0 = \frac{Ltanh\left(\dfrac{W}{L}\right)\left[J_p(0)\left(1+\dfrac{\mu_p}{\mu_n}\right) - J_T\left(\dfrac{\mu_p}{\mu_n}\right)\right]}{2qD_p}\,.$$

Substituting for $P(x = W) = P_0\left[1-\dfrac{x}{W_B}\right]$ as in [5], one gets

$$p(W) = \frac{Ltanh\left(\dfrac{W}{L}\right)\left[J_p(0)\left(1+\dfrac{\mu_p}{\mu_n}\right) - J_T\left(\dfrac{\mu_p}{\mu_n}\right)\right]\left(1-\dfrac{W}{W_B}\right)}{2qD_p}\,. \tag{3-15}$$

The sweeping-out action of charges was applied to find $\dfrac{dV(t)}{dt}$ the turn-OFF analysis

$$I_T = qAp(x)\frac{dW(t)}{dt} \tag{3-16}$$

$$\because W(t) = W_B - W_{bcj}(t)$$

and $$W_{bcj}(t) = \sqrt{\frac{2\varepsilon_{si}V(t)}{qN_B}}$$

$$\therefore \frac{dW(t)}{dt} = -\sqrt{\frac{\varepsilon_{si}}{2qN_B V(t)}} \frac{dV(t)}{dt} \, .$$

From equations (3-15), (3-16) and $P(x = W) = P_0\left[1 - \frac{x}{W_B}\right]$

$$I_T = -qAp(x)\sqrt{\frac{\varepsilon_{si}}{2qN_B V(t)}} \frac{dV(t)}{dt}$$

$$\frac{dV(t)}{dt} = -\frac{I_T}{qAP_0\left(1 - \frac{W}{W_B}\right)}\sqrt{\frac{2qN_B V(t)}{\varepsilon_{si}}}$$

$$\frac{dV(t)}{dt} = \frac{-I_T N_B W_B}{\varepsilon_{si} AP_0} = \frac{-J_T N_B d1}{\varepsilon_{si} P_0} \qquad (3\text{-}17)$$

Ramamurthy et al. [5] used a positive value for $\frac{dW(t)}{dt}$ instead of a negative value which contradicts the equality $W(t) = W_B - W_{bcj}(t)$.

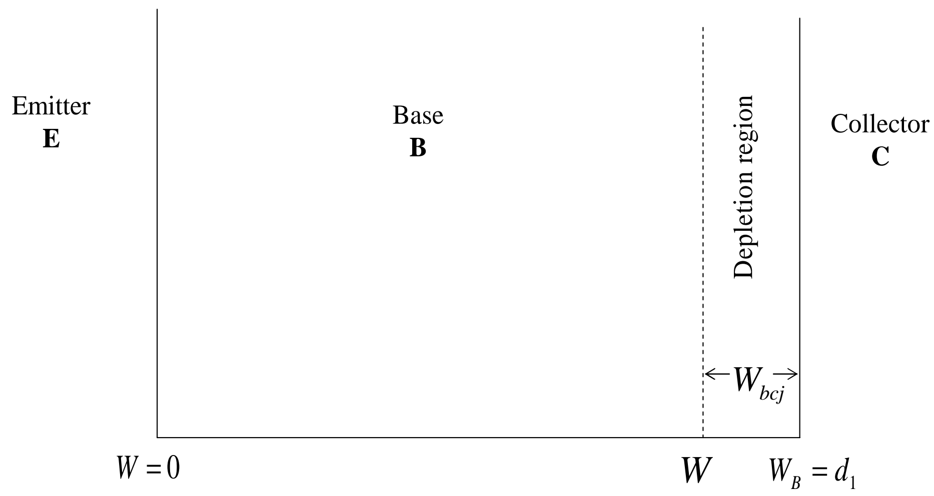

Figure 6 Adjusted coordinate system used for Ramamurthy analysis [5].

4.0 A NEW PHYSICS-BASED TRANSIENT MODEL

4.1 The Steady State

As mentioned in section 2.3.1, the steady state expression for $p(x)$ can be obtained by solving the ambipolar diffusion equation in the base ($\frac{\partial^2 p(x)}{\partial x^2} - \frac{p(x)}{L^2} = 0$) under the boundary conditions [2]

$$p(x = W) = 0 \tag{2-6}$$

$$p(x = 0) = P_0 . \tag{2-7}$$

This equation has the solution of the form

$$p(x) = Ae^{\left(x/L\right)} + Be^{(-x/L)}$$

Solving for the constants A and B, $p(x)$ is expressed as

$$p(x) = P_0 \frac{sinh[(W - x)/L]}{sinh(W/L)} . \tag{4-1}$$

Integrating equation (4-1) and multiplying by qA, the total charge stored Q_0 in the base is obtained as

$$Q_0 = qAP_0 \int_0^W p(x)dx = qAP_0 \left[\frac{cosh(W/L) - 1}{sinh(W/L)} \right]$$

Using the identities $\cosh(2x) = 1 + 2\sinh^2(x)$ and $\sinh(2x) = 2\sinh(x)\cosh(x)$ leads to

$$Q_0 = qALP_0 tanh(W/2L) \quad (4\text{-}2)$$

this Q_0 results from on-state transient.

P_0 which results from the turn-on state, can be calculated by using the general ambipolar transport hole current, the steady state excess carrier distribution equation (4-1), and the following boundary conditions for electron, hole and the total currents

$$I_n(x=0)=0 \quad (4\text{-}3)$$

$$I_p(x=0)=I_T \quad (4\text{-}4)$$

$$\because I_T = I_n + I_p$$

$$\therefore I_T = I_p \,.$$

The assumption of $I_n(0)=0$ is valid for electron carriers in the turn-on state because the quasi-neutral base width ($W = W_B - W_{bcj} \approx W_B$ since $V_{CE} \approx 2.5$ volts) equals the metallurgical base width (W_B). As a result, electrons do not have sufficient time to reach the emitter side of BJT part of IGBT to recombine with the injected hole carriers and constitute electron current.

Using equations (2-4) and (4-1), an expression for P_0 is

$$P_0 = \frac{LI_T(0^-)}{2qAD_p} tanh(W/L) \quad (4\text{-}5)$$

where $I_T(0^-)$ is the steady state turn-on current, which is used as the initial current at the start of turn-OFF period.

Solving equations (4-2) and (4-5), Q_0 can alternatively be expressed as

$$Q_0 = \frac{L^2 I_T(0^-)}{2D_p}[1 - sech(W/L)]. \quad (4\text{-}6)$$

This is the steady state turn-on charge and W is constant in association with Q_0.

For a given $I_T(0^-)$, $(Q_0 - \tau_{HL})$ curves can be produced as shown in Figure 7 for different $I_T(0^-)$ values. As can be seen, Q_0 is proportional to $I_T(0^-)$ and dependent on τ_{HL} through $L^2 = D\tau_{HL}$ that stems from the term $sech(W/L) = sech\left(W/\sqrt{D\tau_{HL}}\right)$. We can also notice that the voltage V in ($W = W_B - \sqrt{\frac{2\varepsilon_{si}V}{qN_B}}$) term corresponds to the steady state voltage across the BJT, which amounts to a value of approximately 2.5 volts.

4.2 Turn-OFF Transient

During the turn-OFF of the IGBT the excess carrier base charge, which was built up during the turn-on, will decay by recombination in the base and by electron current injection into the emitter:

$$\frac{dQ(t)}{dt} = -\frac{Q(t)}{\tau_{HL}} - I_n(0).$$

Assume $\qquad I_n(0) = 0$

The assumption of $I_n(0) = 0$ is valid for electron carriers in turn-OFF transient (gate voltage $\langle V_T$) because the sudden removal of the MOS channel will prevent the attraction of electrons from the p^+ body directly under the gate. As a result, no electron carriers will be available to reach near the emitter part side of BJT part of IGBT to

recombine with the injected hole carriers and constitute electron current.

$$\therefore \frac{dQ(t)}{dt} = -\frac{Q(t)}{\tau_{HL}}$$

this has the solution of the form

$$Q(t) = Q_0' e^{\left(-t/\tau_{HL}\right)} \tag{4-7}$$

where $Q_0' = \alpha F Q_0$ and Q_0 was obtained from the steady state analysis where $p(x) = P_0 \frac{sinh[(W-x)/L]}{sinh(W/L)}$ which is used as an initial condition for the transient analysis. W is almost constant in association with Q_0. As can be seen from Figure 4 region 1, a sudden drop in current from $I_T(0^-)$ to $I_T(0^+)$ will change the magnitude of Q_0 associated with $I_T(0^-)$ to a lower value $Q_0' = \alpha F Q_0$ associated with $I(0^+)$ and F should be less than 1.0. In region 2 where there is a slow decay of current, equation (4-7) applies because that is where recombination takes place.

4.2.1 Expression For $\frac{dV_{CE}(t)}{dt}$

In the turn-OFF period for NPT IGBT since there are no recombination centers, the ambipolar diffusion length is larger than the drift layer which implies $L \rangle\rangle W(t)$ and $W_B \rangle\rangle W(t)$. This is true as carrier lifetimes increase. This is shown if we calculate $L = \sqrt{D \tau_{HL}}$ for different lifetimes and assume $V(t) = V_{BUS} = 400$ volts.

For $\tau_{HL} = 0.3\mu S$, $L = 2.3\times10^{-3}\,cm$, $L = 6.6\times10^{-3}\,cm$ for $\tau_{HL} = 2.45\mu S$ and $L = 1.13\times10^{-2}\,cm$ for $\tau_{HL} = 7.1\mu S$. Since $W = 4.2\times10^{-3}\,cm$, $L \rangle\rangle W(t)$ as carrier lifetimes increase.

The hole distribution is not the same as given by equation (4-1). It can however be estimated by expanding equation (4-1) using Taylor series to yield a first order approximation as

$$p(x,t) = P_0(t)\frac{sinh[(W(t)-x)/L]}{sinh(W(t)/L)}$$

$$sinh[(W(t)-x)/L] = \frac{W(t)-x}{L} + \frac{(W(t)-x)^3}{L^3} + ...$$

$$sinh(W(t)/L) = \frac{W(t)}{L} + \frac{W^3(t)}{L^3} + ...$$

$$p(x,t) = \frac{P_0(t)\left[\frac{(W(t)-x)}{L}\right]}{\frac{W(t)}{L}} = P_0(t)\left[1-\frac{x}{W(t)}\right]$$

$$p(x,t) = P_0(t)\left[1-\frac{x}{W(t)}\right]. \qquad (4\text{-}8)$$

Equation (4-8) is plotted for $p(x)$ as in Figure 8 which shows a linear carrier profile at a given time t. From this Figure the slope ($\frac{\partial P_0}{\partial t} = \frac{-P_0}{W(t)}\frac{dW(t)}{dt}$) is negative since the behavior of $W(t)$ tends towards the minus x-direction as the device voltage $V(t)$ changes with time (moving boundary) [Appendix A].

By integrating equation (4-8) through the base and multiplying by qA, the total charge $Q(t)$ is found as

$$Q(t) = qAP_0(t)\int_0^W p(x,t)dx = \frac{qAW(t)}{2}P_0(t).$$

Using the above equation, the carrier concentration at the emitter edge of the base $P_0(t)$ is related to $Q(t)$ as

$$P_0(t) = \frac{2Q(t)}{qAW(t)} \qquad (4\text{-}9)$$

The accuracy of the voltage waveform in transient is highly correlated to $p(x,t)$. Hence additional improvement on the hole carrier profile is required by substituting equation (4-8) into time dependent diffusion equation ($\frac{\partial^2 p(x,t)}{\partial x^2} = \frac{p(x,t)}{L^2} + \frac{1}{D}\frac{\partial p(x,t)}{\partial t}$), by integrating twice with respect to x, by using the boundary condition $p(x=0,t) = P_0(t)$, $p(x=W,t) = 0$ as well as using the following relation [Appendix A]

$$\frac{\partial P_0(t)}{\partial t} = -\frac{P_0(t)}{W(t)}\frac{dW(t)}{dt}$$

we get

$$\frac{\partial p(x,t)}{\partial x} = \frac{P_0(t)}{L^2}\left(x - \frac{x^2}{2W(t)}\right) + \frac{1}{D}\int\frac{\partial p(x,t)}{\partial t} + C_1.$$

$\frac{\partial p(x,t)}{\partial t}$ comes from equation (4-8) as

$$\frac{\partial p(x,t)}{\partial t} = \frac{\partial P_0(t)}{\partial t}\left(1 - \frac{x}{W(t)}\right) + \frac{P_0(t)x}{W^2(t)}\frac{dW(t)}{dt}.$$

Substituting the above equation in the previous integral yields

$$\frac{\partial p(x,t)}{\partial x}=\frac{P_0(t)}{L^2}\left(x-\frac{x^2}{2W(t)}\right)+\frac{1}{D}\left(\frac{P_0(t)x^2}{W^2(t)}\frac{dW(t)}{dt}-\frac{P_0(t)x}{W(t)}\frac{dW(t)}{dt}\right)+C_1 \qquad (4\text{-}10)$$

Now integrating equation (4-10) with its constant C_1 once with respect to x, we get

$$p(x,t)=\frac{P_0(t)}{L^2}\left(\frac{x^2}{2}-\frac{x^3}{6W(t)}\right)+\frac{1}{D}\frac{dW(t)}{dt}\left(\frac{P_0(t)x^3}{3W^2(t)}-\frac{P_0(t)x^2}{2W(t)}\right)+C_1x+C_2$$

Using the following boundary condition ($p(x=0,t)=P_0(t)$, $p(x=W,t)=0$, we get

$$C_2=P_0(t)$$

$$C_1=\frac{-P_0(t)}{W(t)}-\frac{W(t)P_0(t)}{3L^3}+\frac{1}{6}\frac{P_0(t)}{D}\frac{dW(t)}{dt}$$

$$\therefore\ p(x,t)=\frac{P_0(t)}{L^2}\left(\frac{x^2}{2}-\frac{x^3}{6W(t)}\right)+\frac{1}{D}\frac{dW(t)}{dt}\left(\frac{P_0(t)x^3}{3W^2(t)}-\frac{P_0(t)x^2}{2W(t)}\right)-\frac{P_0(t)x}{W(t)}-\frac{P_0(t)}{L^2}\frac{W(t)x}{3}$$
$$+\frac{1}{6}\frac{P_0(t)x}{D}\frac{dW(t)}{dt}+P_0(t)$$

$$p(x,t)=\frac{P_0(t)}{L^2}\left(\frac{x^2}{2}-\frac{x^3}{6W(t)}\right)-\frac{P_0(t)x}{W(t)}-\frac{P_0(t)W(t)x}{3L^2}+P_0(t)+\frac{1}{D}\frac{dW(t)}{dt}\left(\frac{P_0(t)x^3}{3W^2(t)}-\frac{P_0(t)x^2}{2W(t)}\right)$$
$$+\frac{1}{6}\frac{P_0(t)x}{D}\frac{dW(t)}{dt}$$

$$p(x,t)=P_0(t)\left(\frac{x^2}{2L^2}-\frac{x^3}{6W(t))L^2}-\frac{x}{W(t)}-\frac{xW(t)}{3L^2}+1\right)+\frac{P_0(t)}{W(t)D}\frac{dW(t)}{dt}\left(\frac{x^3}{3W(t)}-\frac{x^2}{2}+\frac{xW(t)}{6}\right)$$

$$p(x,t)=P_0(t)\left(\frac{x^2}{2L^2}-\frac{x^3}{6W(t)L^2}-\frac{x}{W(t)}-\frac{xW(t)}{3L^2}+1\right)+\frac{1}{W(t)D}P_0(t)\frac{dW(t)}{dt}\left(\frac{x^3}{3W(t)}-\frac{x^2}{2}+\frac{xW(t)}{6}\right)$$

$$p(x,t) = P_0(t)\left(1 - \frac{x}{W(t)} + \left(\frac{x^2}{2L^2} - \frac{x^3}{6W(t)L^2} - \frac{xW(t)}{3L^2}\right)\right) + \frac{1}{W(t)}\frac{dW(t)}{dt}\frac{P_0(t)}{D}\left(\frac{x^3}{3W(t)} - \frac{x^2}{2} + \frac{xW(t)}{6}\right)$$

The refined version for the hole distribution during transient is therefore expressed as

$$p(x,t) = P_0(t)\left(1 - \frac{x}{W(t)} + \left(\frac{x^2}{2L^2} - \frac{x^3}{6W(t)L^2} - \frac{xW(t)}{3L^2}\right)\right) - \frac{1}{W(t)}\frac{dW(t)}{dt}\frac{P_0(t)}{D}\left(\frac{x^2}{2} - \frac{W(t)x}{6} - \frac{x^3}{3W(t)}\right) \tag{4-11}$$

Integrating equation (4-11) and multiplying by qA yields the charge $Q(t)$

$$Q(t) = qAP_0(t)\left[\frac{W(t)}{2} - \frac{W^3(t)}{24L^2}\right]$$

Since $L \rangle\rangle W(t)$, the second term can be neglected leading to the previous equation (4-9)

$$P_0(t) = \frac{2Q(t)}{qAW(t)}. \tag{4-9}$$

Substituting for $P_0(t)$ in equation (4-11) leads to $p(x,t)$ as function of $[x, Q(t), W(t)]$.

Equation (4-11) is similar to Hefner's $p(x)$ expression et al. [2] except for three additional terms which modify the linear dependence of p on x.

Since $L \rangle\rangle W(t)$, we substitute for $P_0(t)$ in equation (4-11) by its value from equation (4-9) to calculate $\frac{\partial p(x,t)}{dt}$ expression in the equation of the displacement current $I_n(W)$. The base current $I_n(W)$ is a displacement current in nature and results from the discharge of the reverse-biased collector-base depletion junction capacitance $C_{bcj}(t)$

$$I_n(W) = \frac{d}{dt}(C_{bcj}(t)V_{CE}(t))$$

$$I_n(W) = V_{CE}(t)\frac{dC_{bcj}(t)}{dt} + C_{bcj}(t)\frac{dV_{CE}(t)}{dt}$$

where $$C_{bcj}(t) = \frac{A\varepsilon_{si}}{W_{bcj}(t)} = A\sqrt{\frac{q\varepsilon_{si}N_b}{2V_{CE}(t)}}.$$

Since $$W(t) = W_B - W_{bcj}(t)$$

then $$\frac{dW(t)}{dt} = -\frac{C_{bcj}(t)}{qAN_B}\frac{dV_{CE}(t)}{dt}$$

and the displacement current is

$$I_n(W) = \frac{C_{bcj}(t)}{2}\frac{dV_{CE}(t)}{dt}. \tag{4-12}$$

This type of current flow is usually called the displacement current. The rate of change of $C_{bcj}(t)$ must be included when calculating this current, since the capacitance varies with time as the depletion width change with voltage.

Using equation (4-11), (4-12) and the displacement current equation

$$I_n(W) = \frac{I_T(t)}{1+\frac{1}{b}} + qAD\frac{\partial p(x,t)}{\partial x}\bigg|_{x=W(t)}$$

, $qAD\frac{\partial p(x,t)}{\partial x}\bigg|_{x=W(t)}$ is expressed as

$$qAD\frac{\partial p(x,t)}{\partial x}\bigg|_{x=W(t)} = qADP_0(t)\left[\frac{W(t)}{6L^2} - \frac{1}{W(t)}\right] + \frac{qAP_0(t)}{6D}\frac{dW(t)}{dt}$$

$$\therefore I_n(W) = \frac{C_{bcj}(t)}{2}\frac{dV(t)}{dt} = \frac{I_T(t)}{\left(1+\frac{1}{b}\right)} + qADP_0(t)\left[\frac{W(t)}{6L^2} - \frac{1}{W(t)}\right] + \frac{qAP_0(t)}{6}\frac{dW(t)}{dt} \tag{4-13}$$

$$\because W(t) = W_B - W_{bcj}(t) \text{ and } W_{bcj}(t) = \sqrt{\frac{2\varepsilon_{si}V(t)}{qN_B}}$$

and $$\because C_{bcj}(t) = \frac{A\varepsilon_{si}}{W_{bcj}(t)} = A\sqrt{\frac{q\varepsilon_{si}N_b}{2V(t)}}$$

$$\therefore \frac{dW(t)}{dt} = -\frac{C_{bcj}(t)}{qAN_B}\frac{dV_{CE}(t)}{dt} . \tag{4-14}$$

Substituting equations (4-9) and (4-14) into (4-13) yields the $\frac{dV_{CE}(t)}{dt}$ expression

$$\frac{dV_{CE}(t)}{dt} = \frac{\left[I_T(t) - 4D_p\left(\frac{1}{W^2(t)} - \frac{1}{6L^2}\right)Q(t)\right]}{\frac{C_{bcj}(t)}{2}\left(1+\frac{1}{b}\right)\left[1+\frac{2}{3qAN_BW(t)}Q(t)\right]} \tag{4-15}$$

where $$Q(t) = \alpha F Q_0 e^{\left(-t/\tau_{HL}\right)} \tag{4-7}$$

and $$Q_0 = \frac{L^2 I_T(0^-)}{2D_p}\left[1 - sech(W/L)\right]. \tag{4-6}$$

The fact that the current drops suddenly to $I_T(0^+)$ requires adjusting the initial stored charge to $\alpha F Q_0$ where α is an adjusting parameter and F is a factor that is less than unity derived from reference [2] by assuming $I_n(0) = 0$ [Appendix C] where $F = 2\left(1 - sech\left(\frac{W}{L}\right)\right)/\left(\frac{W}{L}\right)^2$ and W is almost constant in association with Q_0. The output collector-emitter voltage is obtained by simultaneous integration of equations (4-15) and (4-7). W in $sech(W/L)$ term is almost constant since Q_0 is constant.

The anode current is given by

$$I_T(t) = \frac{F I_T(0^-)\left(e^{-t/\tau_{HL}} - e^{-t_1/\tau_{HL}}\right)}{\left(1 - e^{-t_1/\tau_{HL}}\right)} \tag{4-16}$$

and t_1 corresponds to the time t when the output voltage $V_{CE}(t)$ reaches the supply bus voltage.

The above equation applies to the slow decay of current because it is there where recombination takes place while the total current in the ambipolar transport current equation ($I_n(W) = \frac{I_T(t)}{(1+\frac{1}{b})} + qAD\frac{\partial p(x,t)}{\partial t}$) relates the hole current to the displacement current when calculating the anode voltage expression.

It is instructive to note that by multiplying $Q(t)$ by the correction factor αF, the extracted charges in the base are reduced by this factor. The displacement current $C_{bcj}(t)\frac{dV_{CE}(t)}{dt}$ should therefore be also reduced by the same factor αF for scaling purpose in order to account for the reduced charge in the base during the turn-OFF transient.

This new physics-based model has several advantages over Hefner's model:

. The non-linear capacitance is included in the calculation of the displacement current. This is unlike Hefner's model where the capacitance was assumed constant.

. The ambipolar diffusion equation (time-dependent) is totally implemented without neglecting the first part on the right hand side ($\frac{p(x)}{L^2}$) of that equation. However, Hefner et al. [2] did not take this point into account.

. The initial steady state base charge Q_0 for each τ_{HL} can be computed easily in any commercial software programs since the expression for $\frac{dQ(t)}{dt}$ is simpler than Hefner's $\frac{dQ(t)}{dt}$ expression. In the new model, P_0 is not used as an adjusting parameter.

However, in Hefner's model, the initial steady state base charge Q_0 magnitude at different τ_{HL} must be provided separately in the software program since $\frac{dQ(t)}{dt}$ expression is non-linear and has more than one dependent variable ($\tau_{HL}, W(t)$).

. The expression for P_0 is simple and computable due to the boundary conditions. However, P_0 was used as a parameter in Hefner's model and does not have a simple expression.

. The model is not a complex function of the redistribution current (I_R), which is due to the redistribution component of the carrier distribution.

Figure 9 compares the output voltage waveforms for different carrier lifetimes for this model with measured (experimental) data outputs and model in [2] for large inductive loads (10A). Theoretical predictions of the output voltages have been obtained with different carrier lifetimes and compared with experimental data available in the literature and good agreement has been obtained.

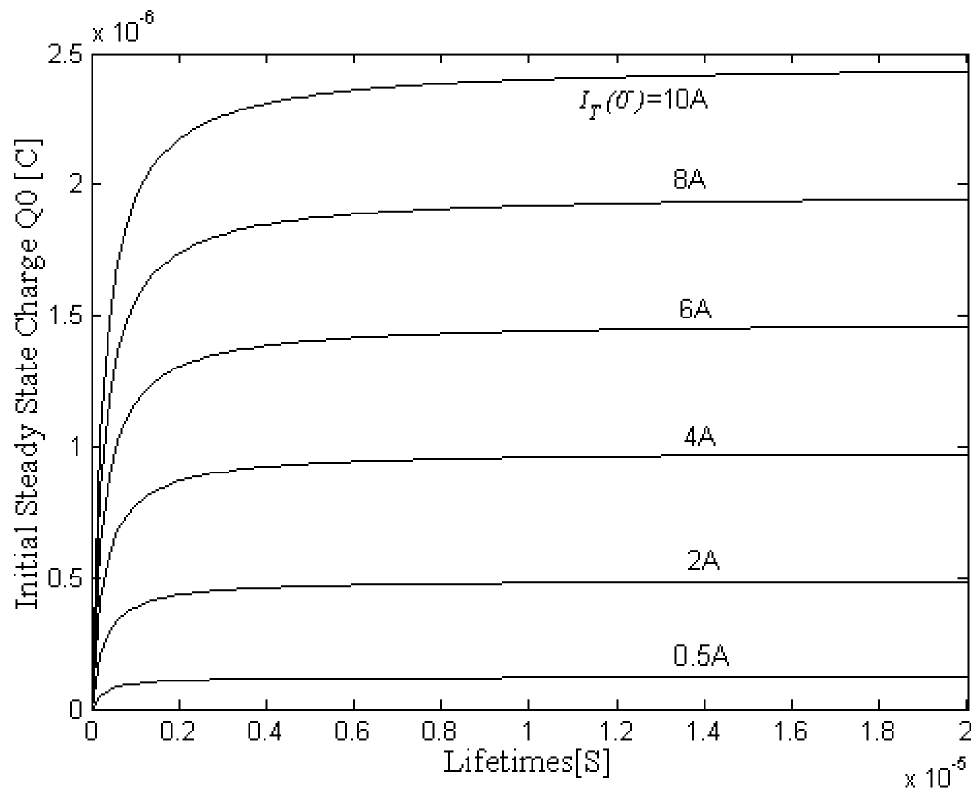

Figure 7 The steady state charge Q_0 as a function of the load current and carrier lifetime τ_{HL}.

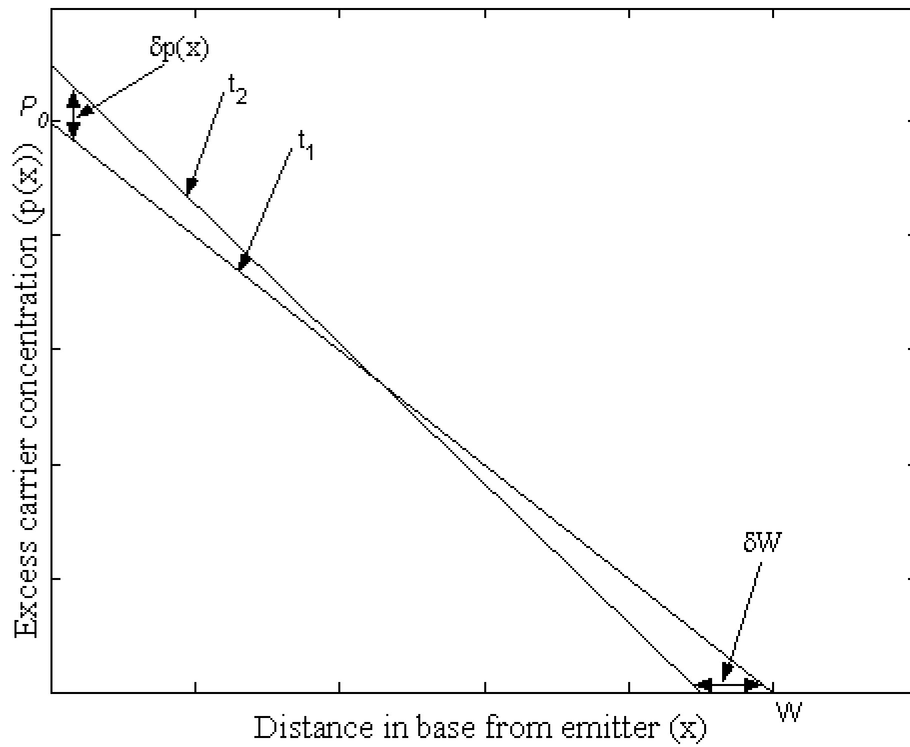

Figure 8 Linear excess carrier concentration profile as a function of distance $W(t)$.

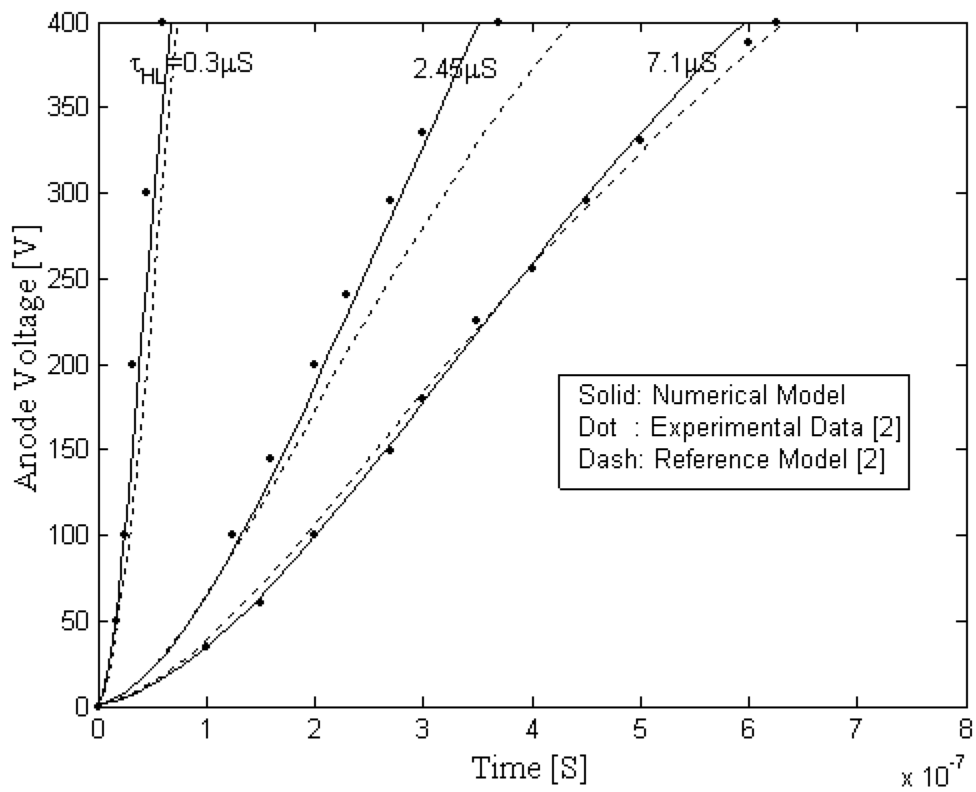

Figure 9 Comparison of anode voltages with the experimental data for different lifetimes.

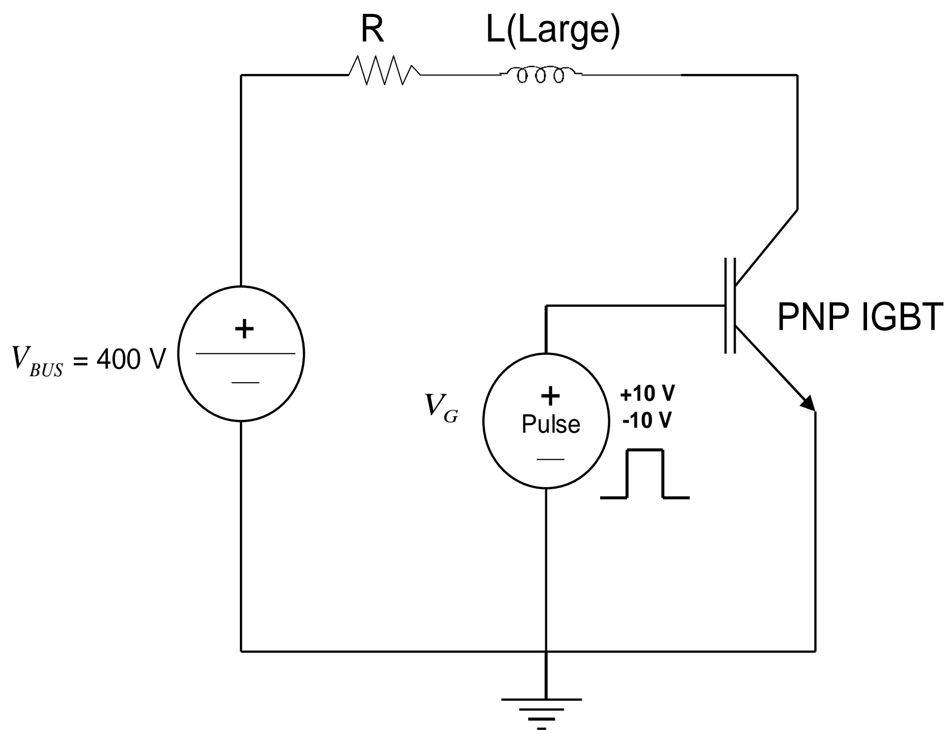

Figure 10 Large inductive loads with no freewheeling diode in an IGBT turn-OFF circuit.

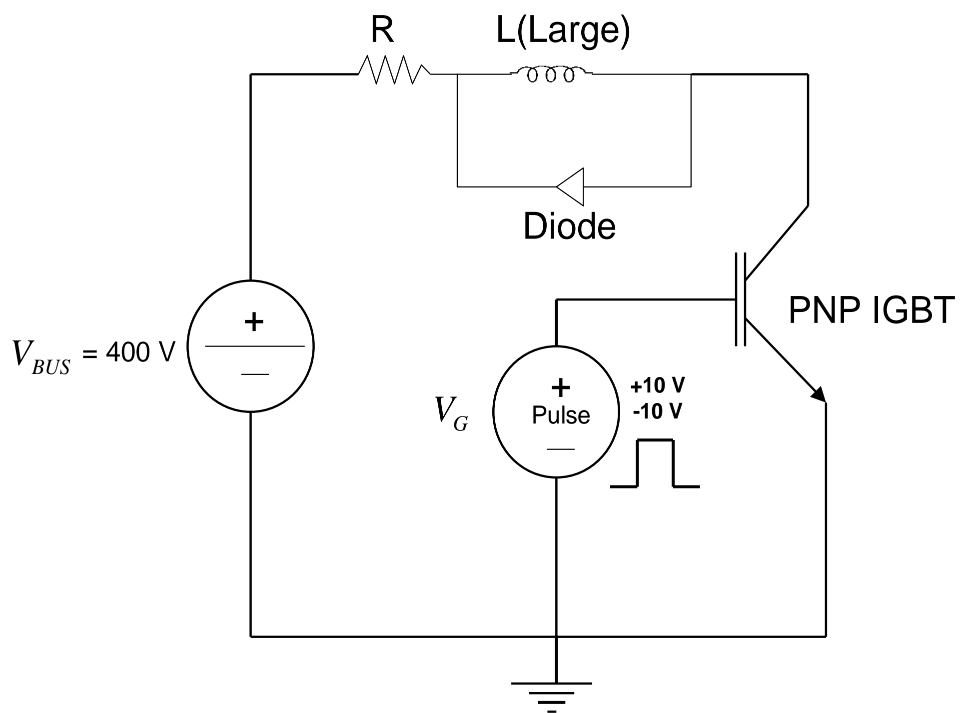

Figure 11 Inductive loads with a freewheeling diode in an IGBT turn-OFF circuit.

Table 1 IGBT Model Parameters

MODEL PARAMETERS	VALUES	UNITS
W_B	$9.3m$	cm
A	0.1	cm^2
N_B	2×10^{14}	cm^{-3}
τ_{HL}	$\tau_{HL} = 0.3\mu S$ -> 10^{13} (**n/** cm^2) $\tau_{HL} = 2.45\mu S$ >10^{12} (**n/** cm^2) $\tau_{HL} = 7.1\mu S$ > **--** (**n/** cm^2)	μS
$D = \frac{2D_n D_p}{D_n + D_p} = \frac{2D_p}{\left(1 + \frac{1}{b}\right)}$	18	cm
L	Varies (τ_{HL} dependent)	cm

Table 2 Physical Parameters

μ_n	1500 cm^2/Vs
μ_p	450 cm^2/Vs
$b = \frac{\mu_n}{\mu_p}$	3.3
n_i	$1.45\times10^{10}\, cm^{-3}$
ε_{si}	$1.05\times10^{-12}\, F/cm$

4.2.2 The Instantaneous Power $P(t)$ and Switching Losses $E_{off}(t)$:

Transient losses occur when switching action takes place in an IGBT. Since the IGBT sustains high anode current density and voltage simultaneously, high power dissipation occurs. The instantaneous power $P(t)$ dissipated by the IGBT is the product of the voltage and the anode current ($V_{CE}(t) * I_T(t)$). From voltage equation (4-15) and current equation (4-16), different power profiles for different device lifetimes τ_{HL} are produced as shown in Figure 12. At higher lifetimes, because of a larger number of carriers, the current is high and as a result the corresponding power dissipation is larger. The transient turn-OFF energy E_{off} results from integrating the instantaneous power over a time interval. For a given value of the device anode current, one data energy point is calculated. The energy results for different device lifetimes are shown in Figures 13, 14 and 15 separately. The comparison of theses energy level losses is shown in Figure 16. To produce E_{off} as a function of the anode current, these energy points for particular anode current values at different device lifetimes are plotted in Figure 17.

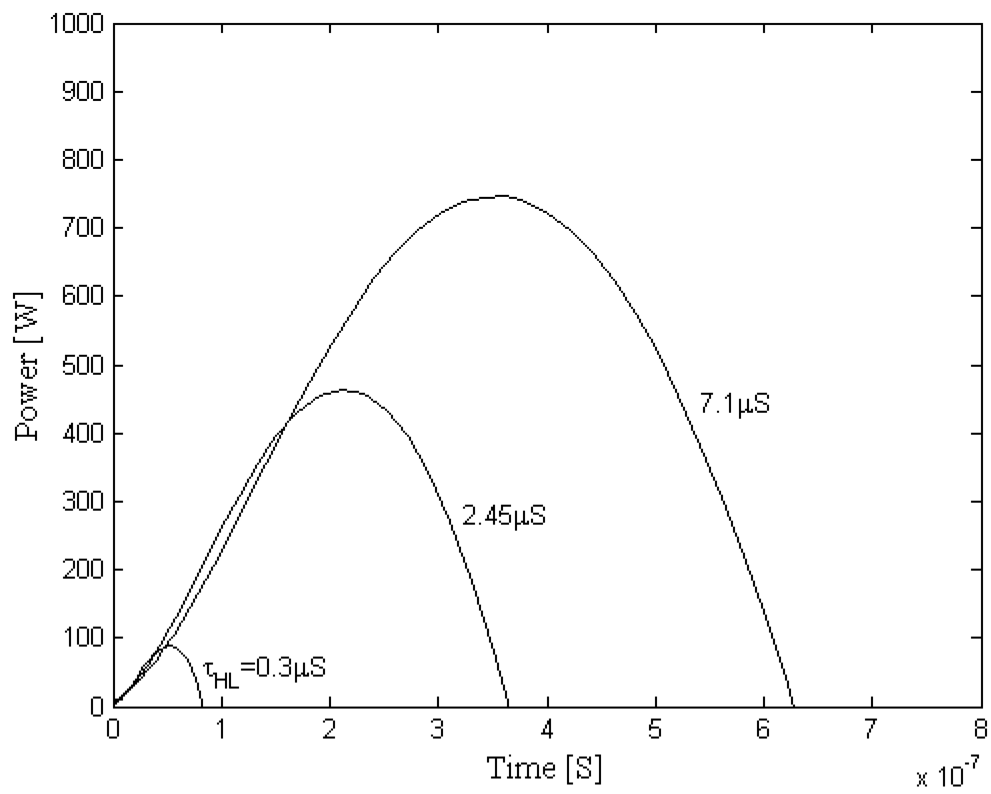

Figure 12 The instantaneous power dissipated by the IGBT for different lifetimes for the numerical model.

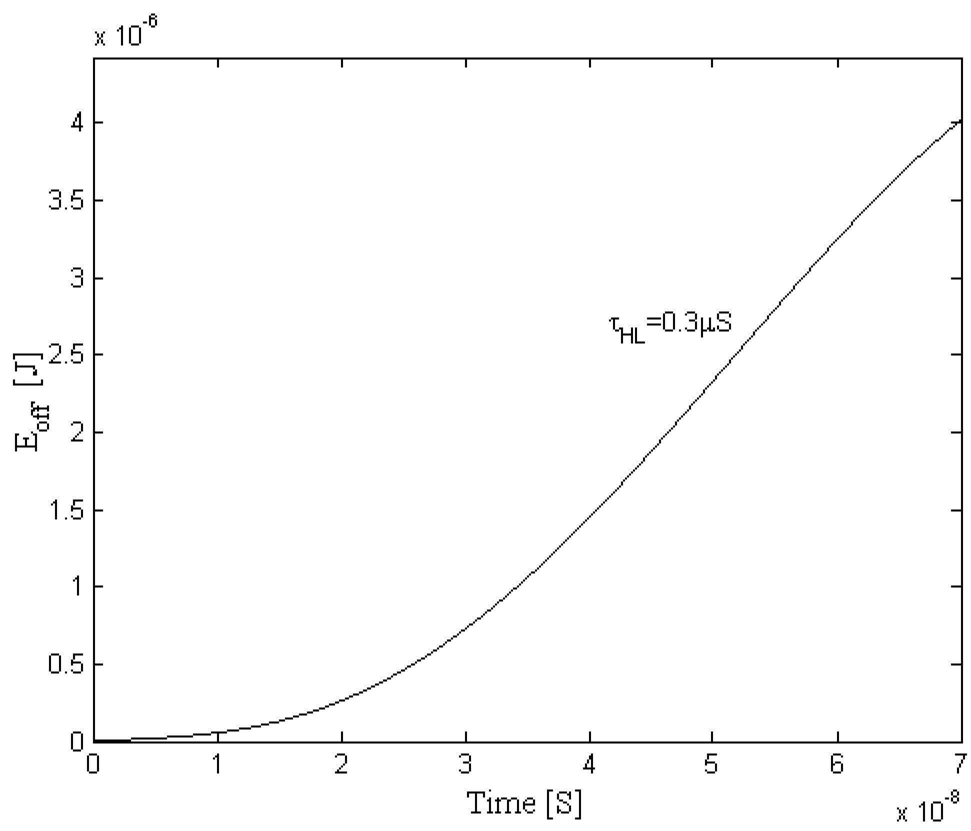

Figure 13 E_{off} as function of time for $\tau_{HL} = 0.3\mu S$

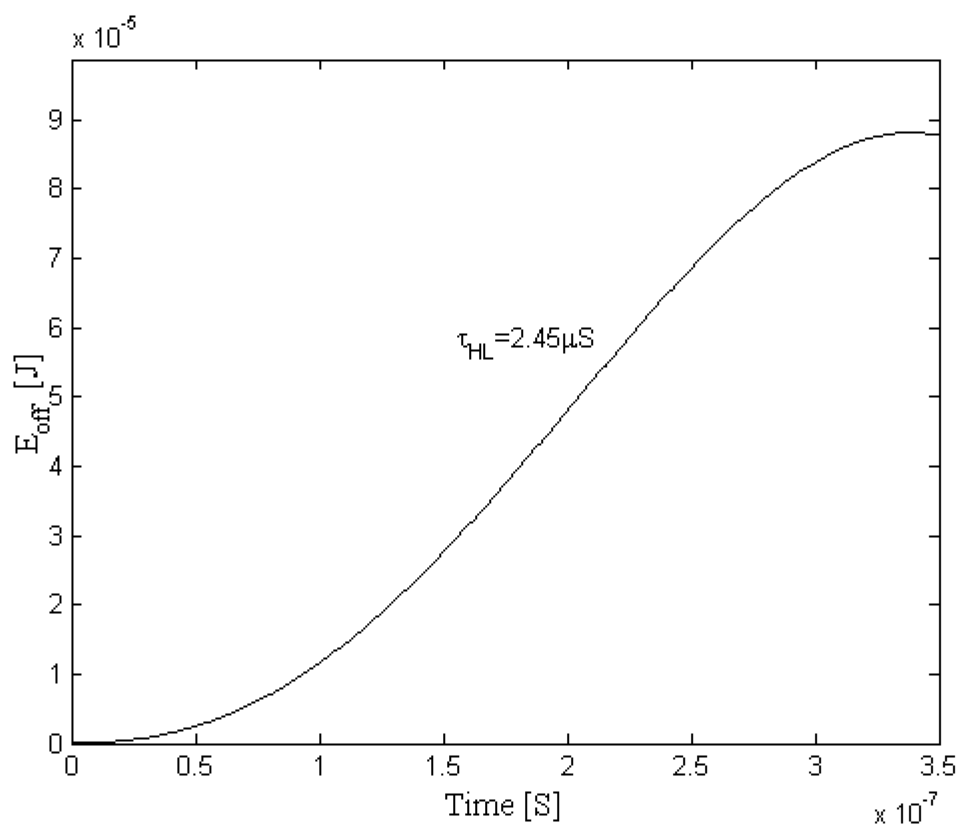

Figure 14 E_{off} as function of time for $\tau_{HL} = 2.45\mu S$.

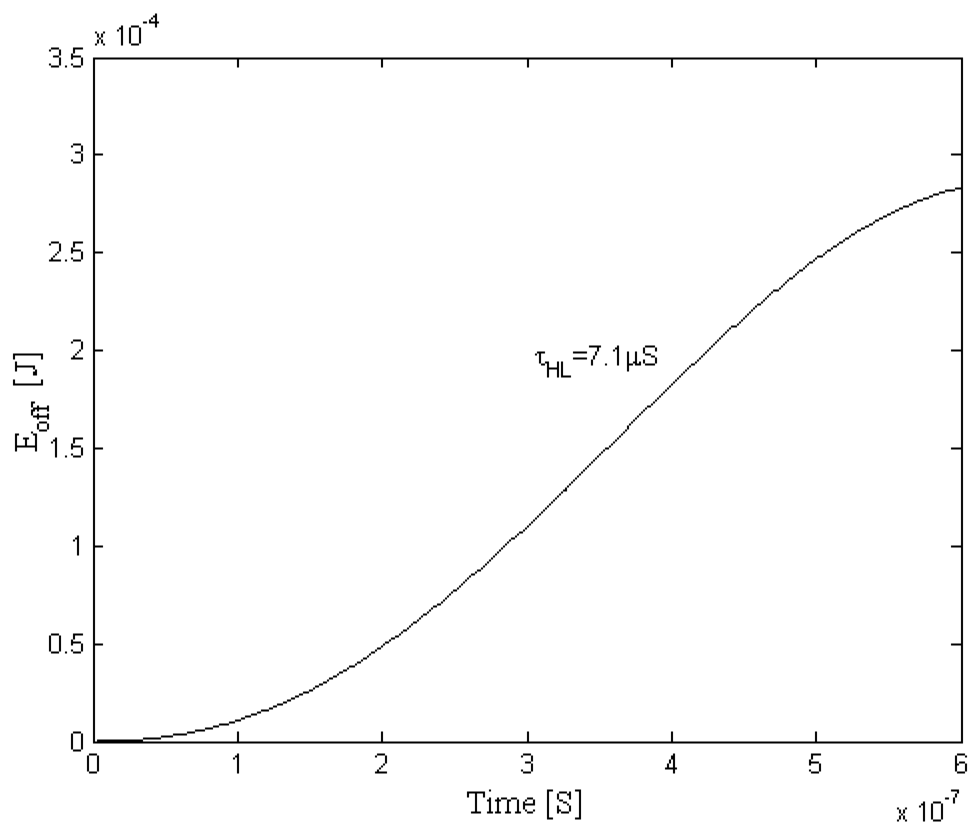

Figure 15 E_{off} as function of time for $\tau_{HL} = 7.1\mu S$.

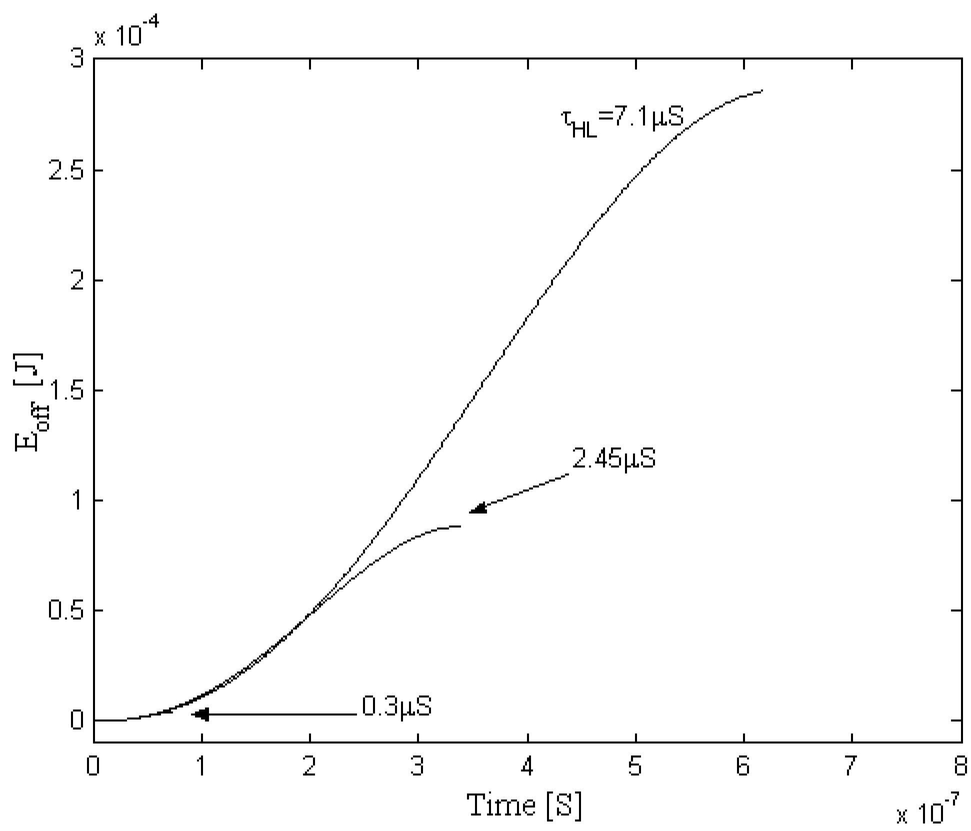

Figure 16 Comparison of the energy losses for three different lifetimes in an IGBT for the numerical model.

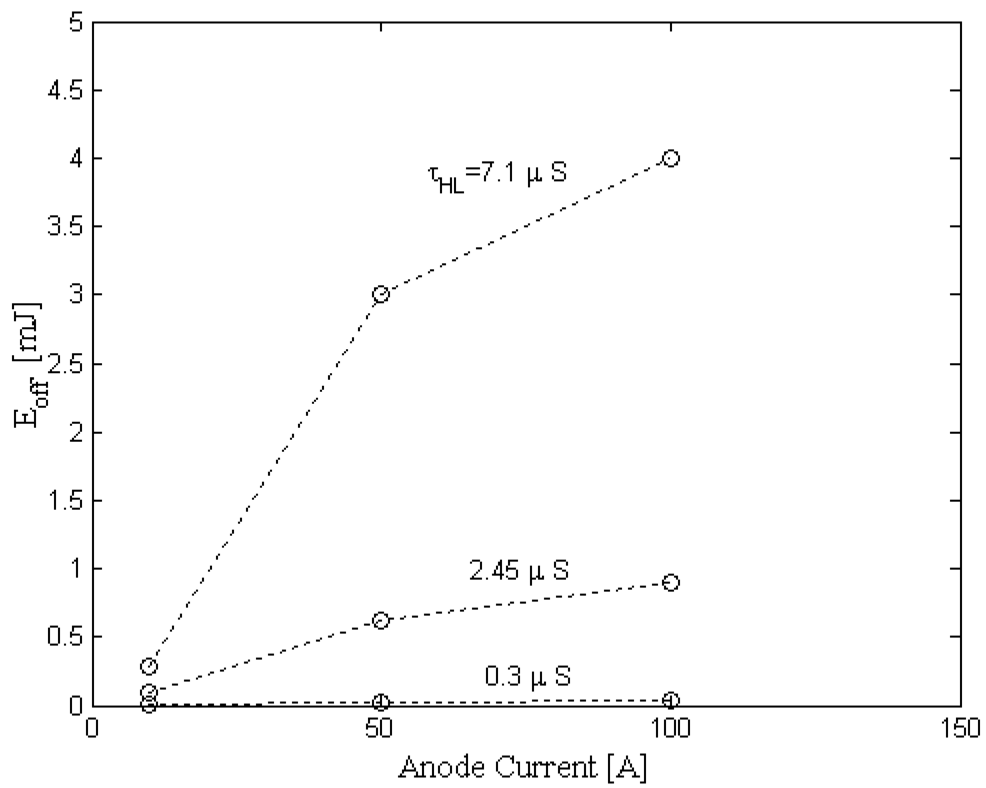

Figure 17 Turn-OFF switching losses (E_{off}) as a function of anode current for the numerical model.

4.2.3 An Alternative Analytical Solution For The Transient $\frac{dV_{CE}(t)}{dt}$:

An alternative analytical solution for the proposed transient turn-OFF of the NPT IGBT is presented. The solution is derived by considering equation (4-15), by assuming an initial solution and using one iteration to obtain a closed form expression for the transient voltage. A constant β is used to adjust the steady state charge Q_0. Based on this approach, the depletion width can be expressed as

$$W_{bcj} = R\sqrt{a_{\max} t} \tag{4-17}$$

where $R = \sqrt{\frac{2\varepsilon_{si}}{qN_B}}$

and $a_{\max}$ is the slope of the initial voltage with time and differs from structures and carrier lifetime.

From equation (4-15), the gradient of anode voltage with time is given as

$$\frac{dV_{CE}(t)}{dt} = \frac{\left[I_T(t) - 4D_p\left(\frac{1}{W^2(t)} - \frac{1}{6L^2}\right)Q(t)\right]}{\frac{C_{bcj}(t)}{2}\left(1+\frac{1}{b}\right)\left[1+\frac{2}{3qAN_BW(t)}Q(t)\right]} \tag{4-15}$$

For the turn-OFF transient, $L \rangle\rangle W(t)$ for which $\frac{1}{L} << \frac{1}{W(t)}$ then equation (4-15) becomes

$$\frac{dV_{CE}(t)}{dt} = \frac{\left[I_T(t) - \frac{4D_p}{W^2(t)}Q(t)\right]}{\frac{C_{bcj}(t)}{2}\left(1+\frac{1}{b}\right)\left[1+\frac{2}{3qAN_BW(t)}Q(t)\right]} \tag{4-18}$$

The above equation can be alternatively be simplified under the assumption that $\frac{2Q(t)}{3qAN_B W(t)} >> 1$ to read

$$\frac{dV_{CE}(t)}{dt} = \frac{\left[I_T(t) - \left(\frac{4D_p}{W^2(t)} \right) \beta Q_0 e^{(-t/\tau_{HL})} \right]}{C_{bcj}(t)\left(1+\frac{1}{b}\right)\left[\frac{\beta Q_0 e^{(-t/\tau_{HL})}}{3qAN_B W(t)} \right]}. \qquad (4\text{-}19)$$

By replacing $\frac{dV_{CE}(t)}{dt} = a_{\max}$ and using the following relations:

$$C_{bcj}(t) = \frac{A\varepsilon_{si}}{W_{bcj}(t)}$$

$$r = A\varepsilon_{si}$$

$$R_r = \frac{r(1+\frac{1}{b})}{3RqAN_B}$$

$$W(t) = W_B - W_{bcj}(t) = W_B - R\sqrt{V_{CE}(t)}$$

equation (4-19) becomes

$$a_{\max} = \frac{I_T(t)}{\frac{\beta R_r Q_0 e^{(-t/\tau_{HL})}}{W(t)\sqrt{V_{CE}(t)}}} - \frac{\frac{4D_p}{W^2(t)}\beta Q_0 e^{(-t/\tau_{HL})}}{\frac{\beta R_r Q_0 e^{(-t/\tau_{HL})}}{W(t)\sqrt{V_{CE}(t)}}}.$$

Multiplying both sides of the above equation by $R_r \beta Q_0 e^{(-t/\tau_{HL})}(W_B - R\sqrt{V_{CE}(t)})t$, collecting terms and doing some algebraic manipulations [Appendix D]; the anode voltage $V_{CE}(t)$ can be obtained as a function of time and charge $Q(t)$ as

$$V_{CE}(t) = \frac{R_B^2 - 2R_A R_C.t - R_B\sqrt{R_B^2 - 4R_A R_C.t}}{2R_A^2} \qquad (4\text{-}20)$$

$$R_A = R(R_r \beta Q_0 e^{(-t/\tau_{HL})} + I(t)R.t)$$

where $$R_B = W_B (R_r \beta Q_0 e^{(-t/\tau_{HL})} + 2I(t)R.t)$$

$$R_C = (W_B^2 I_T(t) - 4D_p \beta Q_0 e^{(-t/\tau_{HL})})$$

Equation (4-20) can be successfully applied to PT IGBT by adding extra terms in $Q(t)$ so that it covers all the IGBTs regardless of structures modified by any reason. In equation (4-20), the value for Q_0 is substituted from equation (4-5). The parameters used for developing the above models are summarized in Tables 1 and 2

The outputs of the analytical model of equation (4-20) for different lifetimes are shown in Figure18. The results are compared with the numerical model and the experimental data [2]. Figure19 shows the anode current profile for $\tau_{HL} = 0.3uS$, $2.45\mu S$ and $7.1\mu S$. The analytical model anode voltage is compared with the numerical one and with the model in [2] in Figure 18 for $\tau_{HL} = 1uS$, $4uS$ and $6uS$ respectively.

Transient losses occur when switching action takes place in an IGBT. Since the IGBT sustains high anode current density and voltage simultaneously, high power dissipation occurs. The instantaneous power $P(t)$ dissipated by the IGBT is the product of the collector-emitter voltage and the anode current ($V_{CE}(t) \times I_T(t)$). The anode current is given by

$$I_T(t) = \frac{F I_T(0^-)\left(e^{-t/\tau_{HL}} - e^{-t_1/\tau_{HL}}\right)}{\left(1 - e^{-t_1/\tau_{HL}}\right)} \qquad (4\text{-}16)$$

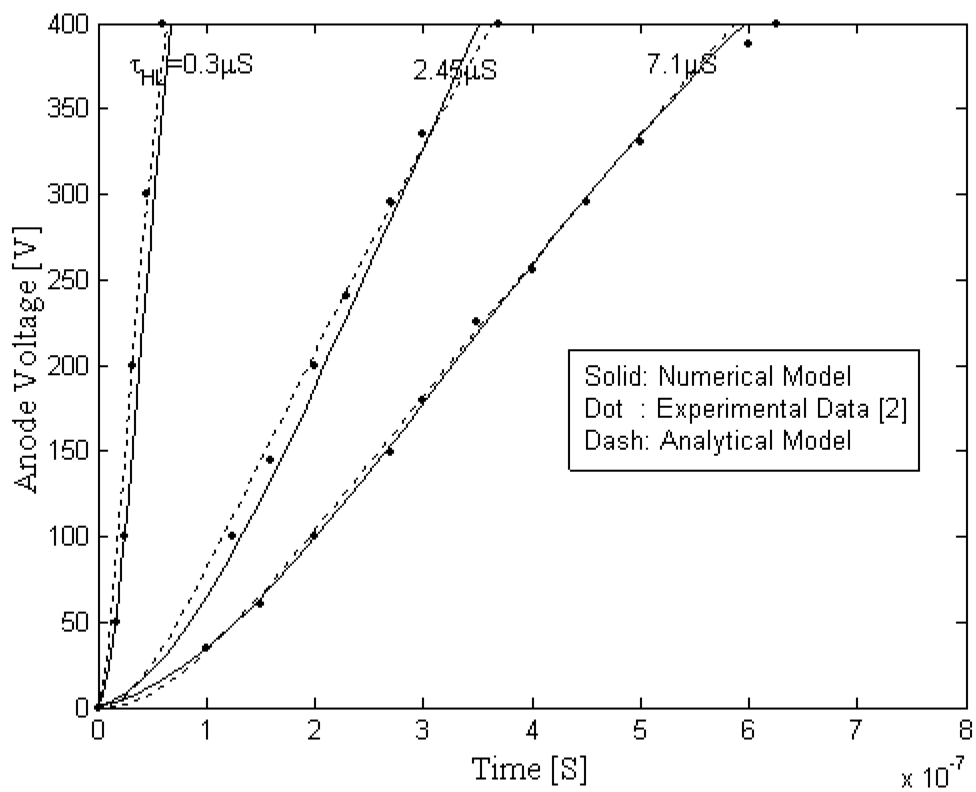

Figure 18 Comparison of anode voltages with different lifetimes for the analytical model and experimental data.

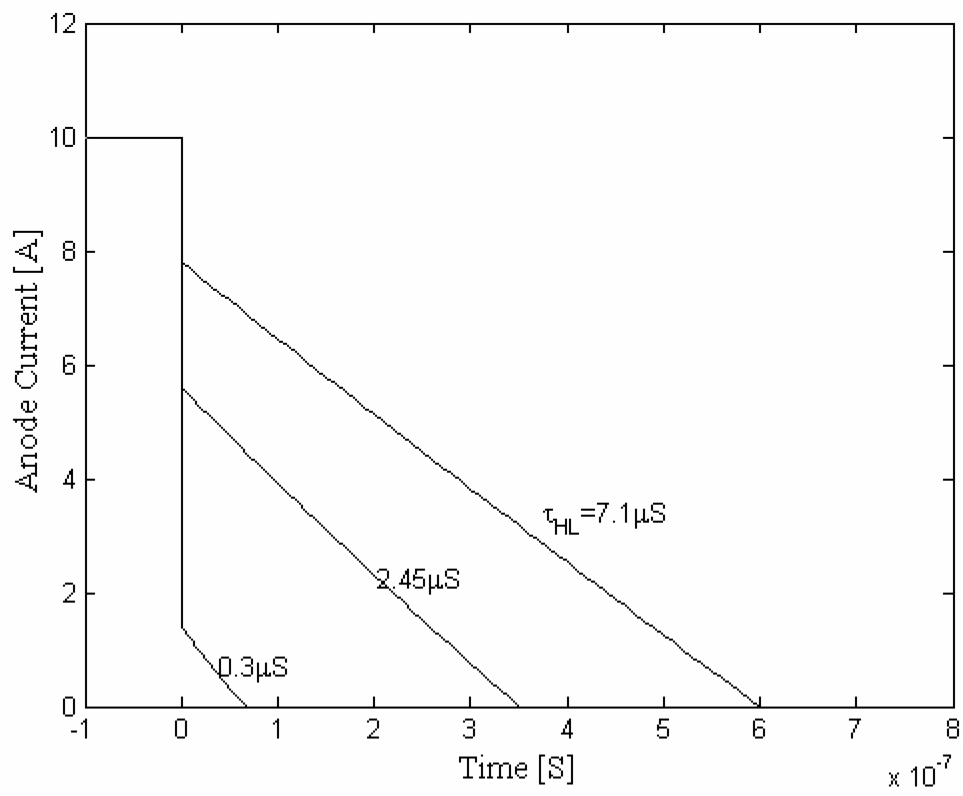

Figure 19 Anode current profiles.

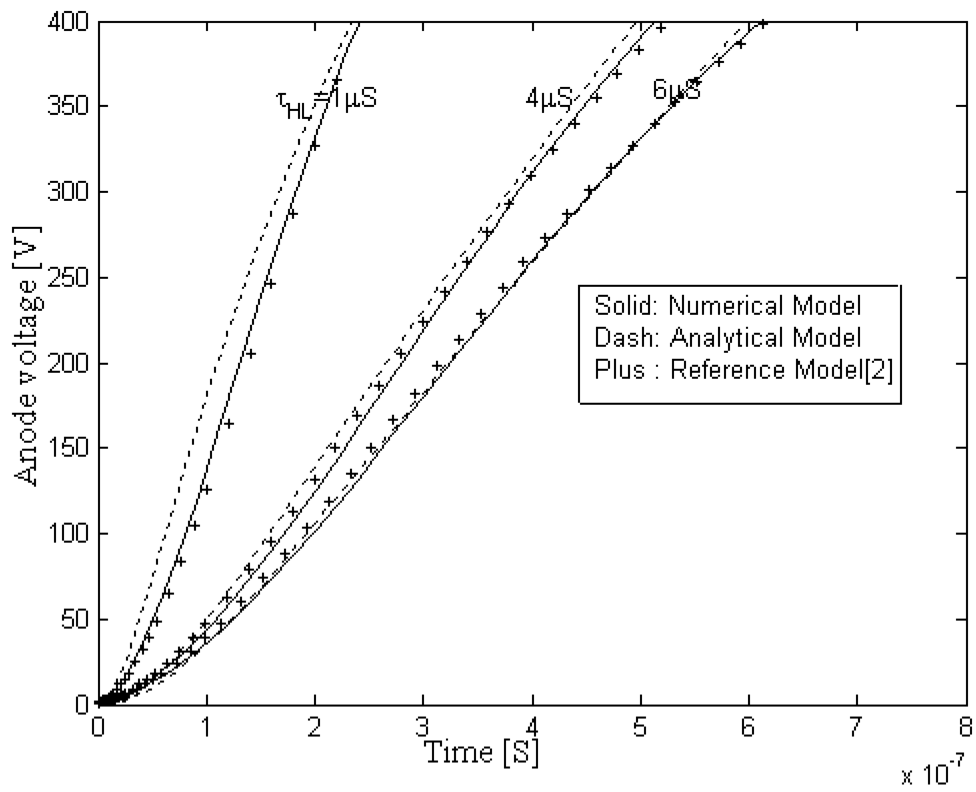

Figure 20 Comparison of anode voltages with the reference model for different lifetimes.

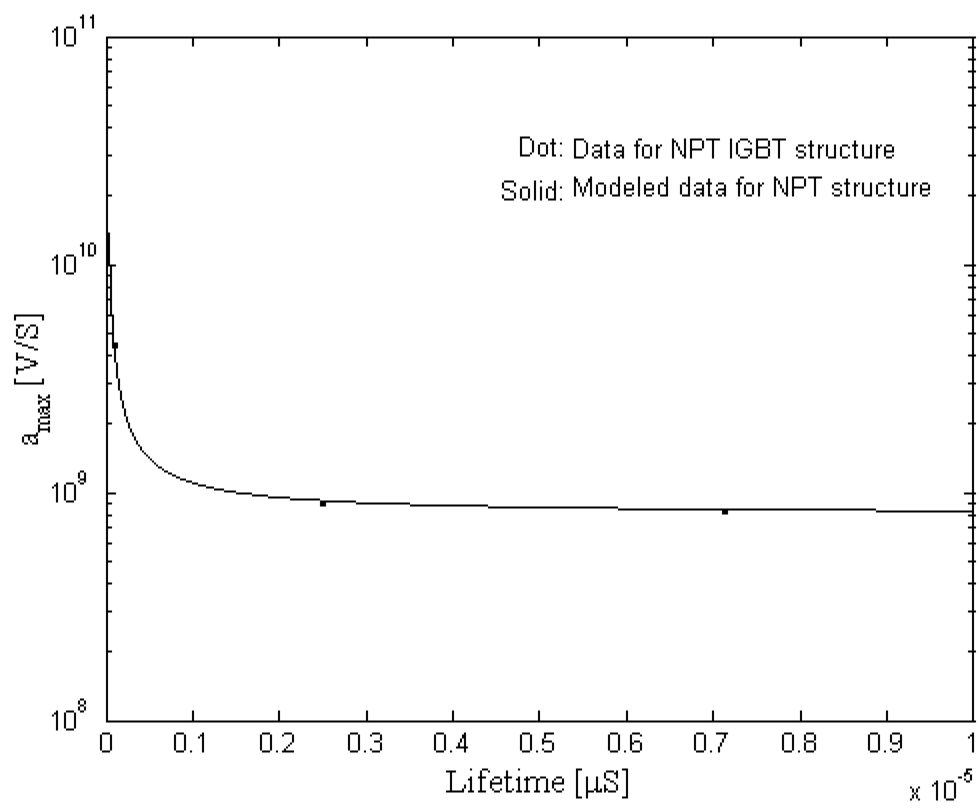

Figure 21 $a_{\max}$ values for different lifetimes for NPT IGBT structure for the analytical model.

5.0 RESULTS AND DISCUSSION

A new physics-based model for NPT IGBT for the transient turn-OFF was developed in chapter 4. The instantaneous power dissipation and the switching energy loss profiles have been produced. An alternative analytical solution for this model has been generated beside a numerical solution.

The numerical anode output voltages are compared with the experimental data and reference model [2] in Figure 9 for 3 different lifetimes $\tau_{HL} = 0.3\mu S, 2.45\mu S$ and $\tau_{HL} = 7.1\mu S$ as measured by Hefner for a device whose parameters are listed in Tables 1 and 2. The output results show good agreement over the wide range of lifetimes. In reference [2], a large inductive load was used in the simulation with no freewheeling diodes. The circuit used is shown in Figure 10. Since the current through an inductor can not change instantaneously, it follows that in this case $I_T(t)$ appearing in equations (4-15) and (4-20) is constant and equal to $I_T(0^-)$. It is instructive to note that the nature of $I_T(t)$ in the model depends on the load condition in the circuit. If the load is purely resistive, the current $I_T(t)$ can not be constant.

The device lifetime determines the output voltage behavior. The injected holes from the emitter of the BJT part of the IGBT get recombined with the electrons coming from the n channel of the MOSFET portion of the IGBT. The excess carrier lifetimes in the base of the IGBT determine the amount of current available in the IGBT. For lower carrier lifetimes, the current is lower as well and, as a result, the output anode voltage

builds up faster and reaches the supply bus voltage. On the other hand, as the carrier lifetime increases, the amount of the produced current increases as well and the output voltage is decreased as shown in Figure 9. The average error between the theoretical predictions of numerical simulation compared with the experimental data for lower carrier lifetimes is within 6% with the accuracy increasing for higher carrier lifetime. The corresponding average error for the analytical model is within 4%. Typical carrier lifetime range is from 1 to 2 μS for practical applications. The new models reveal good agreement for this range. Commercial MATLAB software was used in developing different output results [26].

The instantaneous power dissipation and the switching energy losses in the case of free wheeling diode for different anode currents and lifetimes are shown in Figures 12 and 16. The circuit used is shown in Figure 11. The instantaneous output power is the product of the anode voltage and anode current. The anode current expression (4-16) is used in conjunction with the output voltage to produce the power and energy losses. Figure 19 shows the anode current profiles for three different device lifetimes (τ_{HL}) when using a circuit that has a free wheeling diode in parallel with an inductor. In the turn-ON of IGBT, a steady state current $I_T(0^-)$ flows in the IGBT. At the turn-OFF switching, this steady state current drops initially to a value of $FI_T(0^-)$ then decays exponentially due to the recombination in the base and should reach a zero value at a time $t = t_1$ when the collector-emitter voltage reaches the supply bus voltage. Carrier lifetime determines the exponential decay rate with faster decay when carrier lifetime is smaller. Higher carrier lifetime requires more time for extraction or removal when the device turns-OFF. This power output depends upon the injected carrier lifetime with higher power

dissipation for higher carrier lifetime. From Figure 16, the switching energy losses are the integral of the power output over the time interval. The switching energy losses can also be displayed as function of the anode current I_T as shown in Figure 17. For many commercially available IGBT packages, data are provided for the switching losses as a function of the anode current. The anode current for theses packages ranges from 500 A to 2500 A. However, for lower ranges of anode currents, data are not readily available. The current of Figure 19 has a different decay rate during the turn-OFF for different carrier lifetimes. With lower carrier lifetime, the slope of current decay is very sharp hence the stored base charge extraction is abrupt. As a result, the energy loss is low and visa versa. This confirms the behavior of the switching of energy verses the device anode current. From these results, the power dissipation and energy losses increase with the increase of the carrier lifetime and anode current. The average error of different comparisons is within 5%.

For the alternative analytical solution of the numerical model, the transient behavior of maximum available gradient of voltage $a_{\max}$ is shown in Figure 21. The transient charge $Q(t)$ value is reduced from Q_0 to βQ_0. The depletion width in Q_0 expression comes from equation (4-5) and $a_{\max}$ is lifetime and structure dependent. A value of $\beta = 0.9$ was used to develop the I-V characteristics of the NPT IGBT.

Figure 18 shows an excellent agreement between the alternative analytical model and the experimental data available in literature for the three lifetimes. This confirms the validity of the assumptions made to develop the simple analytical model.

Figure 20 provides additional comparison between the analytical, numerical and data obtained from substituting in the equations of reference [2] since experimental data

are not readily obtainable. The analytical model of [2] with the given parameters can be used as a reference for the comparison since it is the most developed comprehensive model in the literature. From this Figure, the average error for lower carrier lifetime ($\tau_{HL} = 0.3\mu S$) is within 5% with the accuracy increasing for higher carrier lifetime. The outputs are, in general, in good agreement.

6.0 SUMMARY AND FUTURE WORK

This thesis dissertation dealt with the modeling and simulation of the Insulated Gate Bipolar Transistors, which is a preferred power-switching device. A Physics-based model for the NPT IGBT during the turn-OFF period was developed based on the solution of a one-dimensional ambipolar diffusion equation which results from high injection levels of minority hole carriers. The ambipolar transport equations are analyzed in detail. This model was compared with Hefner's model el al. [2] and found to be much simpler and can be implemented easily in commercial software programs. The output predictions are in good agreement with the available literature experimental data.

An analytical solution was introduced in addition to the numerical approach. This approach has a very simple linear form that is easily solvable. The advantage of this model is that it is suitable for and can be applied to different structures of an IGBT (PT IGBT) by applying appropriate charge models.

Since the IGBT sustains high current and voltage simultaneously during the switching-OFF transient, there is high power dissipation in the device. The turn-OFF power dissipation and energy losses were introduced and simulated.

The output characteristics for both the collector-emitter voltage and the anode current can be compared in time point by point and plotted. The interception of the DC line from KCL in a circuit with the produced I-V characteristics will determine the operating point.

The validity of the newly developed models was confirmed by comparison to the available experimental data or the reference model [2].

A future topic of research would be to expand and apply the ideas used in these models to new device structures and then implement them in SABER software simulation to confirm the validity of the developed model compared to the experimental data available in the literature.

APPENDICES

APPENDIX A

LINEAR CHARGE CONTROL

From the steady state analysis we have

$$p(x) = P_0 \frac{sinh[(W-x)/L]}{sinh(W/L)} \tag{A-1}$$

Since the diffusion length (L) is larger than the drift layer thickness (W_B) because of the high lifetime of carriers, one can approximate the carrier profile for the holes $p(x)$ in the drift layer by a linear expression as shown previously

$$p(x,t) \approx P_0 \left[1 - \frac{x}{W(t)}\right]. \tag{A-2}$$

With the aid of the general ambipolar transport hole current expression

$$I_p = \frac{1}{(1+b)} I_T(t) - qAD \frac{\partial p(x)}{\partial x} \tag{A-3}$$

we can find an expression for P_0 from equations (A-2) and (A-3) as

$$\frac{\partial p(x)}{\partial x} = -\frac{P_0}{W(t)} \tag{A-4}$$

$$\because I_n(0) = 0$$

$$\therefore I_p(0) = I_T(t)$$

and $$I_p(0) = I_T(t) = \frac{I_T(t)}{(1+b)} + \frac{2qAD_p}{\left(1+\frac{1}{b}\right)} \frac{P_0}{W(t)}$$

$$I_T(t)\left[1-\frac{1}{(1+b)}\right]=\frac{2qAD_p}{\left(1+\frac{1}{b}\right)}\frac{P_0}{W(t)}$$

$$I(t)=I_T(t=0)=I_T(0^-)$$

$$P_0=\frac{W(t)I_T(0^-)}{2qAD_p} \quad . \tag{A-5}$$

Since total anode current is constant ($I_T(t)=I_T(0^-)$), from the above equation we can find $\frac{\partial P_0}{\partial t}$ as

$$\frac{\partial P_0}{\partial t}=\frac{I_T(0^-)}{2qAD_p}\frac{dW(t)}{dt} \ .$$

Substituting for $I_T(0^-)$ from equation (A-5), the above equation becomes

$$\frac{\partial P_0}{\partial t}=\frac{-P_0}{W(t)}\frac{dW(t)}{dt}. \tag{A-6}$$

From Figure 8 this slope is negative since the behavior of $W(t)$ tends towards the minus x-direction as the device voltage $V_{CE}(t)$ varies with time (moving boundary).

The total charge in the base of the IGBT is

$$Q(t)=qAP_0\int_0^W\left[1-\frac{x}{W(t)}\right]dx=qAP_0\left[x-\frac{x^2}{2W(t)}\right]_0^W$$

$$Q(t)=qAP_0\left[W(t)-\frac{W^2(t)}{2W}\right]$$

$$Q(t)=qAP_0\left[W(t)-\frac{W(t)}{2}\right]$$

$$Q(t)=\frac{qAW(t)P_0}{2}. \tag{A-7}$$

Combining equations (A-5) and (A-7) yields

$$Q(t) = \frac{qAW(t)P_0}{2}$$

$$Q(t) = \frac{qAW(t)}{2}\frac{I_T(t)W(t)}{2qAD_p}$$

$$I_T(t) = \frac{4D_p}{W^2(t)}Q(t)\,. \qquad \text{(A-8)}$$

Equation (A-8) is the linear charge control current and W is constant in this case since $\frac{dV_{CE}(t)}{dt} = 0$. The charge control current (A-8) was derived under much simpler assumptions than Hefner et al. [2].

APPENDIX B

$\frac{I_T(0^+)}{I_T(0^-)}$ EXPRESSION IN CASE $I_n(W)=0$

$I_T(0^+)$ is the current after the initial rapid fall when the IGBT is switched OFF. From the current density of electrons (J_n), the steady state $p(x)$ expression and the fact that $I_n(W)=I_{MOS}=0$ in the turn-OFF case, we can find an expression for $I_T(t=0^+)=I_T(0^+)$

$$J_n(W(t))=\frac{b}{(1+b)}J_T(t)+qD\frac{\partial p(x)}{\partial x}\bigg|_{x=W(t)}$$

or

$$I_n(W(t))=\frac{1}{\left(1+\frac{1}{b}\right)}I_T(t)+\frac{2qAD_p}{\left(1+\frac{1}{b}\right)}\frac{\partial p(x)}{\partial x}\bigg|_{x=W(t)} \qquad \text{(B-1)}$$

and

$$p(x)=P_0\frac{sinh[(W(t)-x)/L]}{sinh(W(t)/L)} \qquad \text{(B-2)}$$

Set $I_n(W)=I_{MOS}=0$

$$\therefore 0=\frac{I_T(t)}{\left(1+\frac{1}{b}\right)}+\frac{2qAD_p}{\left(1+\frac{1}{b}\right)}\frac{\partial}{\partial x}\left[\frac{P_0 sinh[(W(t)-x)/L]}{sinh(W(t)/L)}\right]\bigg|_{x=W(t)}$$

$$\therefore 0=\frac{I_T(t)}{\left(1+\frac{1}{b}\right)}-\frac{2qAD_p}{L\left(1+\frac{1}{b}\right)}\left[\frac{P_0 cosh[(W(t)-x)/L]}{sinh(W(t)/L)}\right]\bigg|_{x=W(t)}$$

$$0=I_T(0+)-2qAD_p\left[\frac{P_0}{Lsinh(W(t)/L)}\right]$$

$$I_T(0^+) = I(0^+) = \left[\frac{2qAD_p}{Lsinh(W(t)/L)}\right]P_0 \,. \tag{B-3}$$

Using equation (4-5) derived previously, $I(0^+)$ and $I_T(0^-)$ are related as

$$\because P_0 = \frac{LI_T(0^-)}{2qAD_p} tanh(W(t)/L) \tag{B-4}$$

$$\therefore I_T(0^+) = I_T(0^-)\frac{tanh(W(t)/L)}{sinh(W(t)/L)} = \frac{I_T(0^-)}{cosh(W(t)/L)} \,. \tag{B-5}$$

Since $cosh(W(t)/L) \rangle\rangle 1$, $I_T(0^+) \langle\langle I_T(0^-)$ as can be seen from Figure 4. Before the reverse bias effect, $W \approx W_B$ and $cosh(W_B/L)$ is constant and much greater than 1.

Equation (B-5) is similar to the expression found in Baliga [1] but with a different and simpler approach for the first time.

Since the current in the large base decays exponentially at a rate determined by the lifetime of hole carriers, $I_T(t)$ can be related to $I_T(0^+)$ as

$$I_T(t) = I_T(0^+)e^{\left(-t/\tau_{HL}\right)} \tag{B-6}$$

where τ_{HL} is the lifetime of the hole carriers.

APPENDIX C

$\frac{I_T(0^+)}{I_T(0^-)}$ EXPRESSION IN CASE $I_n(W) \neq 0$

The steady state base current $I_n(W)$ can be obtained from equations (2-3) and (4-1) of the developed model as

$$I_n(W) = \frac{qP_0AD}{L}\left[\coth(W/L) - \frac{cosh[((W-x)/L)]}{sinh(W/L)}\right]_{x=W} .$$

The steady state anode current $I_p(x = W)$ can be obtained as well from equations (2-4) and (4-1) as

$$I_p(W) = \frac{qP_0AD}{L}\left[\frac{coth(W/L)}{b} + \frac{coth[((W-x)/L)]}{sinh(W/L)}\right]_{x=W} .$$

For the developed model, $I_n(x = 0) = 0$ in which $I_{sne} = 0$, $I_n(W)$ and $I_p(W)$ are expressed as

$$I_n(W) = \frac{qP_0AD}{L}\left[coth(W/L) - \frac{1}{sinh(W/L)}\right] \qquad \text{(C-1)}$$

$$I_p(W) = \frac{qP_0AD}{L}\left[\frac{coth(W/L)}{b} + \frac{1}{sinh(W/L)}\right] . \qquad \text{(C-2)}$$

By adding (C-1) and (C-2) we can get $I_T(0^-)$ (the total steady state anode current) as

$$I_T(0^-) = \frac{qAP_0D}{L}\left(1 + \frac{1}{b}\right)coth(W/L)$$

$$I_T(0^-) = \frac{2qAD_pP_0}{L} coth(W/L). \quad \text{(C-3)}$$

The charge control current for equation (A-8) for ($I_n(x=0)=0$) is

$$I_T(t) = \frac{4D_p}{W^2} Q(t) \quad \text{(C-4)}$$

and the excess stored steady state charge in the base Q_0 was obtained from (4-2)

$$Q_0 = qALP_0 tanh(W/2L). \quad \text{(C-5)}$$

From equation (C-4) and (C-5), an expression for the current immediately after the initial rapid fall in the turn-OFF is

$$I_T(0^+) = \frac{4D_p}{W^2} Q_0 = \frac{4D_p}{W^2} qALP_0 tanh(W/2L)$$

Dividing the above equation by equation (C-3) yields

$$\frac{I_T(0^+)}{I_T(0^-)} = \frac{2[(1 - sech(W/L))]}{(W/L)^2}. \quad \text{(C-6)}$$

This ratio was found to be the correcting factor F .

$$F = \frac{2[(1 - sech(W/L))]}{(W/L)^2} \quad \text{(C-7)}$$

$\frac{I_T(0^+)}{I_T(0^-)}$ is plotted as a function of (W/L) for different lifetimes through L and different V_{BUS}. Figure 22 shows this relation. As τ_{HL} is increased with the increase of V_{BUS}, $\frac{I_T(0^+)}{I_T(0^-)}$ is increased as well. $W(t)$ is a function of the bus voltage.

Figure 23 shows the simulation results compared to the numerical outputs, which show similar trends.

APPENDIX D

DERAVATION OF AN ANALYTICAL SOLUTION FOR $\frac{dV_{CE}(t)}{dt}$

By introducing $V_{CE} = a_{\max}.t$ where $a_{\max}$ represents a time dependent gradient of anode voltage at low transient time and almost constant as the time goes on up to almost $a_{\max}$.

From equation (4-15) and (4-7)

$$\frac{dV_{CE}(t)}{dt} = \frac{\left[I_T(t) - 4D_p\left(\frac{1}{W^2(t)} - \frac{1}{6L^2}\right)Q(t)\right]}{\frac{C_{bcj}(t)}{2}\left(1+\frac{1}{b}\right)\left[1+\frac{2}{3qAN_BW(t)}Q(t)\right]} \quad \text{(D-1)}$$

$$Q(t) = Q_0' e^{\left(-t/\tau_{HL}\right)} \quad \text{(D-2)}$$

where $Q_0' = \beta Q_0$

Equation (D-1) can be alternatively expressed by assuming $\frac{2Q(t)}{3qAN_BW(t)} >> 1$ and substituting for $Q(t)$ expression from equation (D-2) to get

$$\frac{dV_{CE}(t)}{dt} = \frac{\left[I_T(t) - (\frac{4D_p}{W^2(t)})\beta Q_0 e^{(-t/\tau_{HL})}\right]}{C_{bcj}(t)\left(1+\frac{1}{b}\right)\left[\frac{\beta Q_0 e^{(-t/\tau_{HL})}}{3qAN_BW(t)}\right]} \quad \text{(D-3)}$$

By replacing $\frac{dV_{CE}(t)}{dt} = a_{\max}$ or $(V_{CE}(t) = a_{\max} t)$ and using the following relations:

$$C_{bcj}(t) = \frac{A\varepsilon_{si}}{W_{bcj}(t)}$$

$$r = A\varepsilon_{si}$$

$$R_r = \frac{r(1+\frac{1}{b})}{3RqAN_B}$$

$$W(t) = W_B - W_{bcj}(t) = W_B - R\sqrt{V_{CE}(t)}$$

equation (D-3) becomes

$$a_{\max} = \frac{I_T(t)}{\frac{\beta R_r Q_0 e^{(-t/\tau_{HL})}}{W(t)\sqrt{V_{CE}(t)}}} - \frac{\frac{4D_p}{W^2(t)}\beta Q_0 e^{(-t/\tau_{HL})}}{\frac{\beta R_r Q_0 e^{(-t/\tau_{HL})}}{W(t)\sqrt{V_{CE}(t)}}}$$

Multiplying both sides of the above equation by $R_r \beta Q_0 e^{(-t/\tau_{HL})}(W_B - R\sqrt{V_{CE}(t)})t$

$$a_{\max} \cdot t \cdot R_r \beta Q_0 e^{(-t/\tau_{HL})}(W_B - R\sqrt{V_{CE}(t)}) = I(t)\sqrt{V_{CE}(t)}(W_B - R\sqrt{V_{CE}(t)})^2 \cdot t - \sqrt{V_{CE}(t)} \cdot 4D_p \beta Q_0 e(-t/\tau_{HL}) \cdot t$$

From $\frac{dV_{CE}(t)}{dt}$ or $V_{CE}(t) = a_{\max} t$, the above equation becomes

$$V_{CE}(t) \cdot R_r \beta Q_0 e^{(-t/\tau_{HL})}(W_B - R\sqrt{V_{CE}(t)}) = I(t)\sqrt{V_{CE}(t)}(W_B - R\sqrt{V_{CE}(t)})^2 \cdot t - \sqrt{V_{CE}(t)} \cdot 4D_p \beta Q_0 e(-t/\tau_{HL}) \cdot t$$

Dividing both sides of the above equation by $\sqrt{V_{CE}(t)}$, we get

$$\sqrt{V_{CE}(t)} \cdot R_r \beta Q_0 e^{(-t/\tau_{HL})}(W_B - R\sqrt{V_{CE}(t)}) = I(t)(W_B - R\sqrt{V_{CE}(t)})^2 \cdot t - 4D_p \beta Q_0 e(-t/\tau_{HL}) \cdot t$$

$$\begin{aligned} &W_B\sqrt{V_{Ce}(t)} \cdot R_r \beta Q_0 e^{(-t/\tau_{HL})} - V_{CE}(t) R_r \beta Q_0 R \\ &= I(t)(W_B{}^2 - 2W_B R\sqrt{V_{CE}(t)} + R^2 V_{CE}(t)) \cdot t - 4D_p \beta Q_0 e(-t/\tau_{HL}) \cdot t \end{aligned} \tag{D-4}$$

Collecting terms and rearranging for $V_{CE}(t)$ yields

$$(RR_r\beta Q_0 e^{(-t/\tau_{HL})} - I_T(t)R^2 \cdot t)V_{Ce}(t) + (W_B R_r \beta Q_0 e^{(-t/\tau_{HL})}$$
$$+ 2I(t)W_B R \cdot t)\sqrt{V_{CE}(t)} + (-I_T(t)W_B{}^2 + 4D_p \beta Q_0 e(-t/\tau_{HL})) \cdot t = 0$$

Multiplying by the negative sign and rearranging to get

$$R(R_r \beta Q_0 e^{(-t/\tau_{HL})} + I_T(t)R \cdot t)V_{CE}(t) - W_B(R_r \beta Q_0 e^{(-t/\tau_{HL})} +$$
$$2I(t)R \cdot t)\sqrt{V_{CE}(t)} + (I_T(t)W_B{}^2 - 4D_p \beta Q_0 e(-t/\tau_{HL})) \cdot t = 0 \qquad \text{(D-5)}$$

Using the notations below

$$R_A = R(\beta R_r Q_0 e^{(-t/\tau_{HL})} + I_T(t)R \cdot t)$$

$$R_B = W_B(R_r \beta Q_0 e^{(-t/\tau_{HL})} + 2I_T(t)R \cdot t)$$

$$R_C = (I_T(t)W_B^2 - 4\beta D_p Q_0 e^{(-t/\tau_{HL})})$$

the discriminant $= b^2 - 4ac = (R_B^2 - 4 \cdot tR_A R_C)$, then equation (D-5) becomes

$$R_A V_{CE}(t) - R_B\sqrt{V_{CE}(t)} + R_C \cdot t = 0$$
$$R_A\sqrt{V_{CE}(t)}\sqrt{V_{CE}(t)} - R_B\sqrt{V_{CE}(t)} + R_C \cdot t = 0$$

and has the solution of the form

$$\sqrt{V_{CE}(t)} = \frac{-(-R_B) \pm \sqrt{(-R_B)^2 - 4R_A R_C \cdot t}}{2R_A}$$
$$= \frac{R_B \pm \sqrt{-R_B{}^2 - 4R_A R_C \cdot t}}{2R_A}$$

Squaring the above equation, we get the final analytical form

$$V_{CE}(t) = \frac{R_B^2 \pm 2R_B\sqrt{R_B^2 - 4R_A R_C \cdot t} + R_B^2 - 4R_A R_C \cdot t}{4R_A^2}$$

$$V_{CE}(t) = \frac{R_B^2 - 2R_A R_C \cdot t \pm R_B\sqrt{R_B^2 - 4R_A R_C \cdot t}}{2R_A^2}$$

$$V_{CE}(t) = \frac{R_B^2 - 2R_A R_C \cdot t - R_B \sqrt{R_B^2 - 4R_A R_C \cdot t}}{2R_A^2} \tag{D-6}$$

where

$$R_A = R(\beta R_r Q_0 e^{(-t/\tau_{HL})} + I(t)R.t)$$

$$R_B = W_B(\beta R_r Q_0 e^{(-t/\tau_{HL})} + 2I(t)R.t)$$

$$R_C = (W_B^2 I_T(t) - 4\beta D_p Q_0 e^{(-t/\tau_{HL})})$$

Equation (D-6) is the analytical form of equation (4-15) and can be easily plotted for different lifetime with the appropriate $a_{\max}$ value.

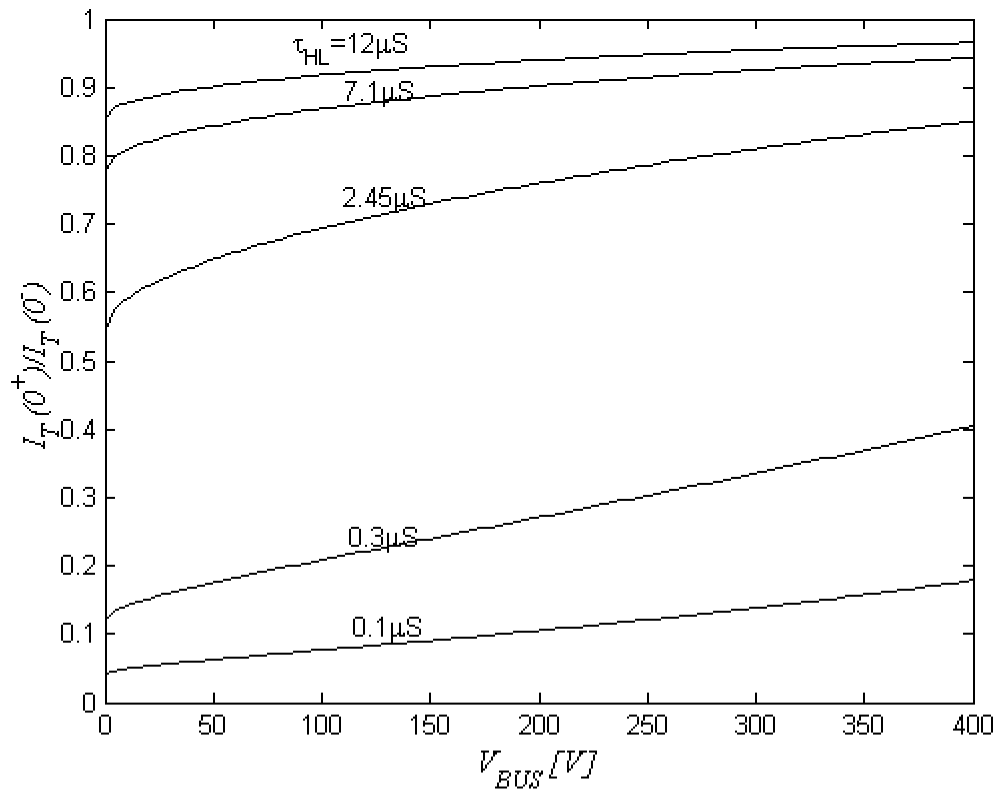

Figure 22 $\frac{I_T(0^+)}{I_T(0^-)}$ as a function of the bus voltage and lifetime through the ratio of $\left(W(t)/L\right)$.

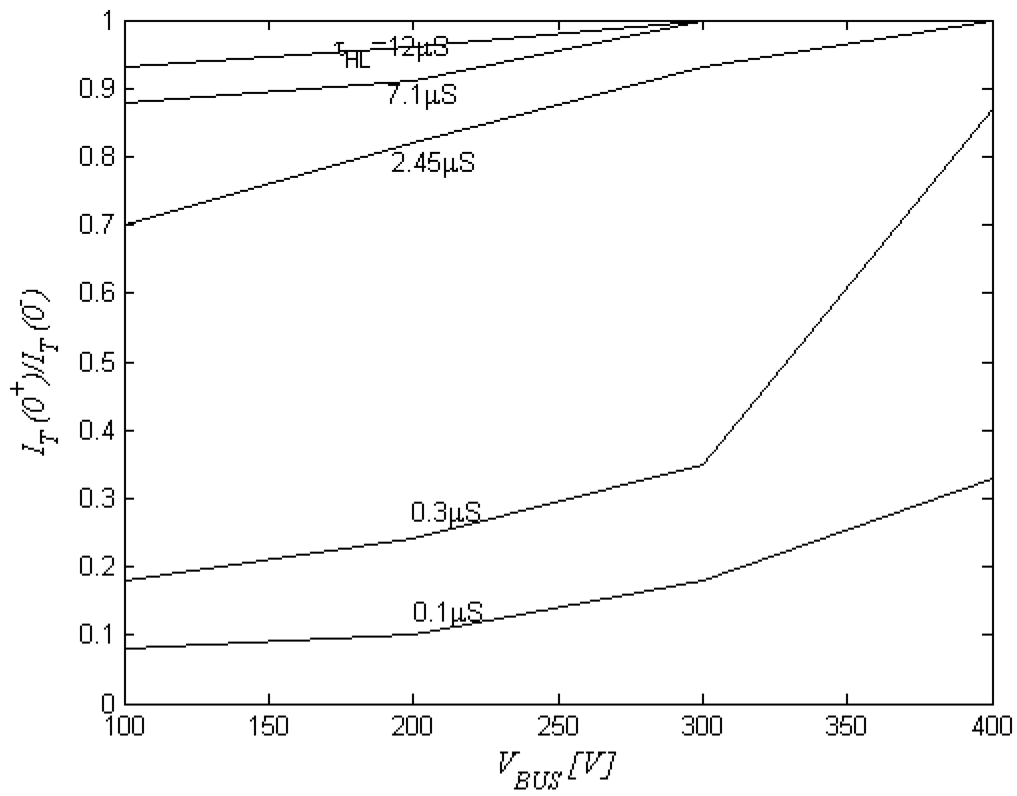

Figure 23 Saber software simulation for $I_T(0^+)$ as a function of V_{bus} and τ_{HL}.

BIBLIOGRAPHY

BIBLIOGRAPHY

1. Baliga B.J., "Power Semiconductor Devices", PWS Publishers, ch. 8, Boston (1996).

2. A.R. Hefner and D.L. Blackburn, "An Analytical Model for the Steady State and Transient Characteristics of the Power Insulated-Gate Bipolar Transistor", Solid-State Electronics Vol.31, pp. 1513-1532, 1988.

3. A.R. Hefner, "Analytical Modeling of Device-Circuit Interactions for the Power Insulated Gate Bipolar Transistor (IGBT)", IEEE Transactions on Industry Applications, Vol.26, No.6, Nov/Dec 1990.

4. Malay Trivedi, Krishna Shenai, "Modeling the Turn-OFF of IGBT's in Hard and Soft-Switching Applications", IEEE Transactions on Electron Devices, vol.44, pp.887-893, May 1997.

5. A. Ramamurthy, S. Sawant, and B.J. Baliga,"Modeling the $\left[\frac{dV}{dt}\right]$ of the IGBT during Inductive Turn-OFF", IEEE Transactions on Power Electronics, Vol.14, No.4, July 1999.

6. B. Fatemizadeh and D. Silber, "A Versatile Model for IGBT including Thermal Effects", 24th IEEE Power Electronics Specialists Conf. (PESC'93), Seattle, USA, June 20-25, 1993, pp. 85-92.

7. Y. Yue, J.J. Liou, and I. Batarseh, "A Steady-State and Transient Model Valid for all Free-Carrier Injection Conditions", 12th IEEE Applied power Electronics 1997.

8. J. Sgg, P. Tuerkes and R. Kraus, "Parameter Extraction Methodology and Validation for an Electro-Thermal Physics-Based NPT IGBT Model", IEEE Industry Applications Society Annual Meeting, New Orleans, Louisiana, October 1997, pp. 1166-1173.

9. D.S. Kuo, C. Hu, and S.P. Sapp, "An Analytical Model for the Power Bipolar MOS Transistor", Solid-State Electronics, Vol.29, No.12, pp. 1229-1237, 1986.

10. K. Sheng, S.J. Finney, and B.W. Williams, "A new Analytical IGBT Model with Improved Electrical Characteristics", IEEE Transactions on Power Electronics, Vol.14, pp.98-107, Jan. 1999.

11. K. Sheng, Barry W. Williams and Stephen J. Finney, "A Review of IGBT Models", IEEE Transactions on Power Electronics, Vol.15, No.6, November 2000, pp. 1250-1266.

12. Philippe Luturcq," A Study of Distributed Switching Processes in IGBTs and Other Power Bipolar Devices", IEEE 28th Annual Power Electronics Specialists Conference, Vol.1, pp. 139-147, 1997.

13. Naresh Thapar and Baliga, Jayant B., "An experimental Evaluation of the On-State Performance of the Trench IGBT Designs", Solid-State Electronics Vol. 42, No. 5, pp. 771-776, 1998.

14. Udrea F. and Amartunga G.S.J., "An On-State Analytical Model for the Trench IGBT", Solid-State Electronics Vol. 41, No. 8, pp. 1111-1118, 1997.

15. Chong-Man Yun Doo, Young Kim, Min-koo Han and Yearn-Ik Choi, "Numerical Analysis of a New Vertical IGBT Structure with Reduced JFET Effect", Solid-State Electronics Vol. 39, No. 8, pp. 1179-1183, 1996.

16. Robinson Andrew L., Pattanayak Deva N., adler, Michael S., baliga, B. Jayan, and wildi, Eric J., "Lateral Insulated Gate Transistors with Improved Latchup Characteristics", IEEE Device Letters, Vol. EDL-7, No. 2, February, 1986.

17. Darwish M. and Board K., "Lateral Resurfed COMFET", Electronics Letters, Vol. 20, No. 12, pp. 519-520, 1984.

18. Deva N. Pattanayak, A.L. Robinson, T. Paul Chow, Michael S. Adler, B. Jayant Baliga and Eric J. Wildi, "n-Channel Lateral Insulated Gate Transistors: Part I- Steady-State Characteristics", IEEE Trans. On Electron Devices, Vol. ED-33, No. 12, pp. 1956-1963, 1986.

19. Fossum Jenny G. and Kim Yeong-Seuk, "static and Dynamic Latchup in the LIGBT", IEEE Trans. On Electron Devices, Vol. 35, N0. 11, pp. 1977-1985, 1998.

20. Vellvehi M., Godignon P., Flores D., Fernandez J., Hidalgo S., Rebollo J. and Millan J., "A New Lateral IGBT for High Temperature Operation", Solid-State Electronics Vol. 41, No. 5, pp. 793-747, 1997.

21. Ravishankar S. and B. Jayant Baliga, "Analysis of On-State Carrier Distribution in the DI-LIGBT", Solid-State Electronics, Vol. 41, No. 5, pp. 733-738, 1997.

22. Sunkavalli Ravishankar and Baliga B. Jayant, "Composition of High Speed DI-LIGBT Structures", Solid-State Electronics, Vol. 41, No. 12, pp. 1953-1956, 1997.

23. Huang Qun and Amaratunga Gehan, "Forward Blocking Capability of Double Gate IGBTs at High Temperatures", Solid-State Electronics, Vol. 38, No. 5, pp. 981-982, 1995.

24. Robert F. Pierret, "Semiconductor Device Fundamentals", Addison-Wesley Publishing Company, Inc, pp. 75-148, 1996.

25. Ben G. Streetman, "Solid State Electronic Devices", Prentice-Hall, Inc., Englewood Cliffs, New Jersey (1980), chaprter11.

26. MATLAB User's Manual.